Cell

Gut Immune Maturation Depends on Colonization with a Host-Specific Microbiota

Hachung Chung,[1,2] Sünje J. Pamp,[3,6] Jonathan A. Hill,[2,8] Neeraj K. Surana,[1,2,7] Sanna M. Edelman,[1,2] Erin B. Troy,[1,2] Nicola C. Reading,[1,2] Eduardo J. Villablanca,[4] Sen Wang,[4] Jorge R. Mora,[4] Yoshinori Umesaki,[5] Diane Mathis,[2] Christophe Benoist,[2] David A. Relman,[3,6] and Dennis L. Kasper[1,2,*]

[1]Channing Laboratory, Brigham and Women's Hospital
[2]Department of Microbiology and Immunobiology
Harvard Medical School, Boston, MA 02115, USA
[3]Departments of Microbiology and Immunology and of Medicine, Stanford University School of Medicine, Stanford, CA 94305, USA
[4]Department of Medicine, Gastrointestinal Unit, Massachusetts General Hospital, Harvard Medical School, Boston, MA 02114, USA
[5]Yakult Central Institute for Microbiological Research, Yaho 1796, Kunitachi, Tokyo 186-8650, Japan
[6]Veterans Affairs Palo Alto Health Care System, Palo Alto, CA 94304, USA
[7]Division of Infectious Diseases, Children's Hospital Boston, Boston, MA 02115, USA
[8]Present address: Tempero Pharmaceuticals, Cambridge, MA 02139, USA
*Correspondence: dennis_kasper@hms.harvard.edu
DOI 10.1016/j.cell.2012.04.037

SUMMARY

Gut microbial induction of host immune maturation exemplifies host-microbe mutualism. We colonized germ-free (GF) mice with mouse microbiota (MMb) or human microbiota (HMb) to determine whether small intestinal immune maturation depends on a coevolved host-specific microbiota. Gut bacterial numbers and phylum abundance were similar in MMb and HMb mice, but bacterial species differed, especially the Firmicutes. HMb mouse intestines had low levels of $CD4^+$ and $CD8^+$ T cells, few proliferating T cells, few dendritic cells, and low antimicrobial peptide expression—all characteristics of GF mice. Rat microbiota also failed to fully expand intestinal T cell numbers in mice. Colonizing GF or HMb mice with mouse-segmented filamentous bacteria (SFB) partially restored T cell numbers, suggesting that SFB and other MMb organisms are required for full immune maturation in mice. Importantly, MMb conferred better protection against *Salmonella* infection than HMb. A host-specific microbiota appears to be critical for a healthy immune system.

INTRODUCTION

Mutually beneficial host-microbe interactions shaped by eons of coevolution take place in all orders of life. In humans, the nutrient-rich intestinal environment is inhabited by up to 100 trillion microbes, the vast majority of which are nonpathogenic bacteria essential to human health. Recognition of the importance of microbes to human physiology has led to studies aimed at defining what bacterial species or genes compose a healthy human microbiota (HMb) (Arumugam et al., 2011; Turnbaugh et al., 2007). Identification of microbes on the basis of small subunit (16S) ribosomal RNA (rRNA) gene sequences has substantially elucidated the gut microbiota's composition. Analyses of the gut microbiota of vertebrates, including humans, have shown that Firmicutes and Bacteroidetes predominate among the >80–100 bacterial phyla on Earth (Eckburg et al., 2005). In the phyla represented, abundant species and strains are found. The HMb is similar to the microbiotas of other mammals at the phylum level but distinct at the species and strain levels (Dethlefsen et al., 2007). Despite vast individual variation in species and strains, a person's gut microbiota more resembles that of other people than that of other mammals (Ley et al., 2008a).

Work in germ-free (GF) mice, which display developmental defects including abnormal nutrient absorption and altered intestinal morphology and motility (Smith et al., 2007), has shown that the gut microbiota is critical for intestinal immune maturation. GF animals have smaller Peyer's patches (PPs), fewer plasma cells, fewer intraepithelial lymphocytes (IELs), impaired antimicrobial peptide and IgA secretion, and other immunologic deficiencies (Round and Mazmanian, 2009); many deficiencies are corrected by recolonization with a health-associated mouse commensal microbiota. Gut microbiota-stimulated immune maturation maintains gut homeostasis by protecting the host from infections (Duan et al., 2010), injury (Rakoff-Nahoum et al., 2004), and damaging inflammatory responses (Atarashi et al., 2011; Mazmanian et al., 2008). Exclusivity between the host and specific symbiotic bacteria has been studied in invertebrate models. In the squid *Euprymna scolopes*, *Vibrio fischeri* is central to tissue development (Koropatnick et al., 2004). In tsetse flies, *Wigglesworthia glossinidia* enhances host fitness, and flies are sterile in its absence (Pais et al., 2008). In complex mammals, it remains unclear whether

health-associated development depends on specific bacterial species exclusive to the host.

Different host species are colonized with different bacterial consortia (Ley et al., 2005). Reciprocal gut microbiota transplantation between zebrafish and mice shows that the host gut habitat selects for certain microbial community structures (Rawls et al., 2006). Diet and host phylogeny are both critical determinants of gut bacterial diversity (Ley et al., 2008b; Ochman et al., 2010). Despite broadened knowledge of factors determining the shape and composition of the gut bacterial community, it is not clear whether the community typically colonizing a given mammalian host species preferentially stimulates a specific program of immune maturation. Have mammals (like invertebrates such as the squid and the fly) coevolved with specific bacterial species uniquely capable of stimulating immune maturation? In other words, is mammalian immune maturation dependent on the mere presence of bacteria, or is a host-specific microbiota required?

To address these questions, we colonized GF mice at birth with a mouse gut microbiota (MMb) or a human gut microbiota (HMb). We studied immune maturation and gut microbiota composition over time by deep pyrosequencing of 16S rRNA genes. MMb and HMb mice share the same major bacterial phyla, but their microbiotas (particularly the Firmicutes) differ significantly at the operational taxonomic unit (OTU) level. MMb and HMb result in remarkably different small intestinal immune systems. Absolute cell numbers and gene transcription in the small intestine indicate that innate and adaptive immune maturation in mice colonized with an HMb (comparable in bacterial abundance to the MMb) resembles that in GF mice. Moreover, HMb mice are more susceptible than MMb mice to gastrointestinal infection. This observation suggests that mammalian hosts have coevolved with a specific consortium of bacterial species that stimulates intestinal immune maturation.

RESULTS

GF Swiss Webster (SW) mice underwent oral gavage with pooled fecal specimens from two healthy humans or with fecal/cecal contents from specific pathogen-free (SPF) SW mice. The two groups of recipient mice were then maintained in separate gnotobiotic isolators. To mimic age-dependent changes in the gut microbiota (Palmer et al., 2007) and the immune system (Chassin et al., 2010; Olszak et al., 2012), we bred mice in the isolator, naturally exposing the offspring to maternal microbes during and after birth (Figure 1A). Both MMb and HMb offspring had a smaller cecum than GF mice, whose cecum is abnormally large (see Figure S1A available online). Body weight did not differ in age-comparable MMb and HMb offspring (Figure S1B).

Fecal Microbiota of MMb and HMb Mice

To monitor the evolution of gut microbial communities in these previously GF mice, we pyrosequenced bar-coded, amplified bacterial 16S rDNA in fecal samples from MMb and HMb parent mice (P0) and their first (F1) and second (F2) offspring generations (Figure 1A). MMb and HMb mice displayed similar relative abundances of major intestinal bacterial phyla, with Bacteroidetes predominating and Firmicutes and Proteobacteria next most abundant (Figure 1B). Quantitative PCR (qPCR) of bacterial 16S rRNA genes and quantitative aerobic and anaerobic culture of bacteria (Figure S1C) showed a similar total bacterial load in MMb and HMb mice.

MMb and HMb mice shared most taxa at the genus level within the Bacteroidetes (e.g., *Bacteroides*, *Parabacteroides*, *Prevotella*, and *Alistipes*); however, the relative abundance of these taxa drastically differed between MMb and HMb mice, closely resembling the patterns in their respective inocula (Figure 1C). MMb and HMb mice shared many Firmicute classes and families (Figure 1D), with the predominant Lachnospiraceae and Ruminococcaceae accompanied by members of the genera *Bacillus* in MMb mice and *Clostridium* 2 in HMb mice. Again, these patterns closely resembled those in the respective inocula. Similarly, MMb and HMb mice shared many genera of Proteobacteria but with different relative abundance resembling the patterns in the respective inocula (Figure 1E). Closer examination of major bacterial phyla at the species (OTU) level revealed striking differences in Firmicutes. Of 1,321 Firmicute-affiliated OTUs, only 20 (1.5%) were shared by MMb and HMb mice. This figure was significantly higher in other major bacterial phyla (Bacteroidetes, 33.7%; Proteobacteria, 43.4%; Figures 1F and S1D; Table S1). MMb and HMb inocula had similar patterns of OTU overlap, with the least overlap (0.8%) in the Firmicutes (Figure S1E). Of OTUs in the mouse inoculum, 7% were not detected in MMb mice; of those in the human inoculum, 30% were not detected in HMb mice. The majority of absent OTUs were low-abundance Firmicute taxa (Tables S2A and S2B). In addition, we found taxa in six fecal specimens from three healthy humans (Dethlefsen and Relman, 2011) that were lacking in HMb mice; most were Firmicutes (Table S2C).

Differences and similarities between microbial communities are revealed by determination of unweighted UniFrac distances, which take into account the presence/absence and evolutionary relatedness of OTUs, and by subsequent principal coordinate analysis. The first principal coordinate (P1), which explained 59% of variance in the data, separated MMb from HMb mouse samples and showed relatively small differences within MMb and HMb mouse samples. The second principal coordinate (P2) showed a high degree of similarity among all MMb mouse samples (including the mouse inoculum); however, the two human inocula had a community distinct from that of HMb mouse samples (Figure 1G). Samples from P0 HMb mice were widely separated along the P2 axis, and an apparently unstable transition state contrasted with the rather stable state in the F1 and F2 generations. Intriguingly, the same pattern was observed when only the Firmicute-affiliated OTUs were taken into account (Figure 1H), a result indicating that members of the Firmicutes are responsible for most observed differences in gut community between MMb and HMb mice and for the apparent instability in the HMb P0 generation. The analyses suggested that MMb and HMb mice have similar total bacterial loads and similar relative abundances of the major bacterial phyla in the gut but differ significantly in bacterial species, especially Firmicutes. The implication is that Firmicutes, in particular, show host specificity.

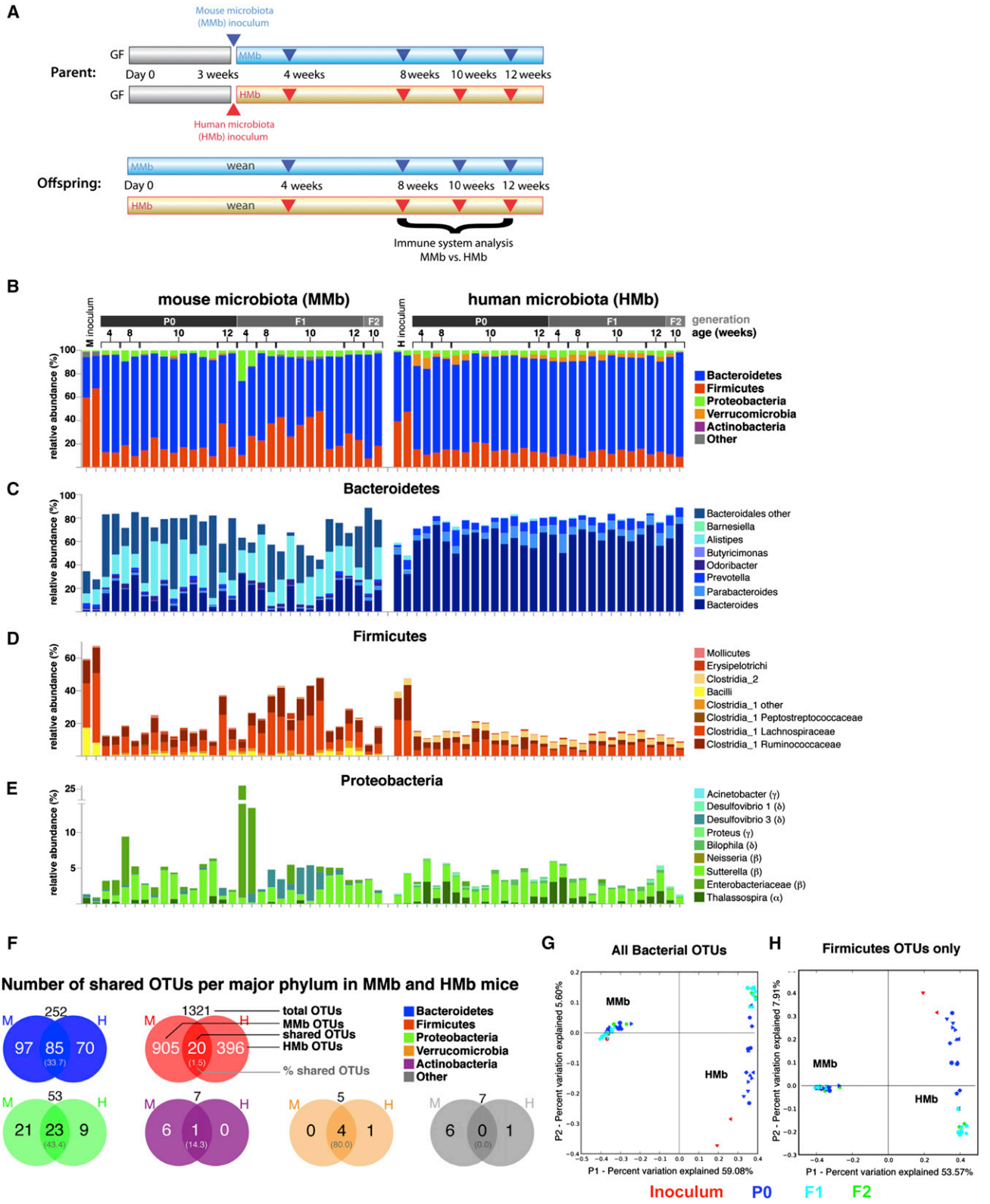

Figure 1. MMb and HMb Mouse Gut Microbiotas Are Similar in Major Bacterial Phyla Abundance with Differences at the OTU Level

(A) Schematic of colonization model (see text for details) is illustrated. Blue and red arrowheads indicate fecal pellet collection for bacterial 16S rDNA sequencing. Offspring were sacrificed for immune system analysis.

MMb, but Not HMb, Mice Exhibit Expansion of Adaptive and Innate Intestinal Immune Cells

Although MMb colonization of GF mice reverses many intestinal immune abnormalities (Smith et al., 2007), it is not clear whether an HMb can do so. To determine how bacterial species-level differences affect intestinal immune maturation, we measured absolute numbers of T cells in the small intestinal lamina propria (LP). As expected, GF mice had few T cells in the LP, and MMb colonization brought LP T cell numbers closer to those in SPF mice. Despite prolonged exposure to diverse bacteria from birth, HMb offspring were deficient in total numbers and percentages of T cells ($CD4^+$ and $CD8^+$) in the small intestinal LP; this deficiency unexpectedly resembled that in GF mice (Figures 2A and S2A). Next, we examined T cell numbers in the small intestinal IEL compartment; the MMb is known to expand IELs expressing the $\alpha\beta$ T cell receptor ($\alpha\beta$TCR), but not those expressing the $\gamma\delta$TCR (Bandeira et al., 1990). MMb mice had a significantly higher percentage and total number of $\alpha\beta$TCR IELs and a higher $\alpha\beta$TCR/$\gamma\delta$TCR ratio than did HMb and GF mice (Figures 2B, S2A, and S2B). The deficient T cell numbers in HMb mouse small intestines were confirmed by immunohistochemistry (Figure 2C). Similar to their offspring, HMb P0 mice had lower T cell numbers in the IEL and LP compartments than MMb P0 mice (data not shown).

We asked whether the deficiency in T cell numbers in HMb offspring was restricted to intestinal tissue or was broader, involving secondary intestinal lymphoid organs such as PPs and mesenteric lymph nodes (MLNs). PPs sample antigens directly from the gut lumen and are important in initiating gut immune responses. Consistent with reports that PP organogenesis begins in the embryonic stage in the absence of microbes (Eberl et al., 2004), we found no difference in PP numbers along the intestines of SPF, MMb, HMb, and GF mice (Figure 3A). Moreover, the percentages of $CD3^+$ T cells in PPs of MMb and HMb mice were comparable (Figure S3A). Despite the latter similarity, the PPs of MMb mice were visibly larger than those of HMb mice and contained significantly more total $CD4^+$ and $CD8^+$ T cells (Figures 3B, 3C, and S3B). PPs of SPF mice contained more T cells than did PPs of MMb mice; this difference suggested that, upon artificial transfer of MMb to GF mice, some PP-stimulatory mouse bacterial species may have been lost. MLNs, which drain cells from PPs and intestinal tissue, also contained higher percentages and numbers of T cells in MMb mice than in HMb mice (Figures 3D, S3A, and S3C). In contrast to differences found in the small intestine, no difference in large intestinal LP $CD3^+$ and $\alpha\beta$TCR IEL numbers was found among SPF, MMb, HMb, and GF mice. However, large intestinal $\gamma\delta$TCR IEL numbers were higher in SPF and MMb mice than in HMb and GF mice (Figure S3D). These data suggest that the microbiota regulates T cell populations in the small and large intestines via distinct mechanisms.

The deficient T cell numbers in HMb mice were limited to the intestine; MMb and HMb offspring did not differ in terms of T cell numbers in the spleen, inguinal lymph nodes, or brachial lymph nodes (Figures 3E and S3E). To assure that the differences in gut T cell numbers between MMb and HMb mice were neither artifactual nor due to inadequate HMb sample numbers, we collected fecal samples from ten additional human donors. GF mice colonized with these fecal samples had lower gut T cell numbers than GF mice colonized with the mouse inoculum (Figure 3F). In all four gut compartments (LP, PPs, MLNs, and IELs), these mice had T cell numbers comparable to those in mice colonized with the original human inoculum.

Dendritic cells (DCs)—$CD11c^+$ innate immune cells—are critical regulators of downstream T cell responses and interact closely with gut bacteria by sampling the intestinal lumen (Kelsall and Rescigno, 2004). DC numbers (defined by $CD11c^{high}$ expression) in small intestinal LP tissue were similar in MMb and HMb mice (Figure S3F). In contrast, in PPs and MLNs, HMb and GF mice had lower numbers of DCs than did MMb mice (Figure S3F). Antimicrobial peptides constitute another critical arm of innate intestinal immunity, providing protection from bacterial penetration of the gut (Vaishnava et al., 2011). MMb colonization induced gene expression of *RegIII*γ, an antimicrobial peptide produced by gut epithelial cells, but HMb was deficient in upregulating *RegIII*γ (Figure S3G).

Thus, regardless of exposure to large bacterial numbers with a phylum representation similar to that in MMb mice, HMb mice have very low levels of intestinal T cells, DCs, and antimicrobial peptide expression. These immunologic parameters indicate that the adaptive and innate small intestinal immune system of the HMb mouse—despite the diverse colonizing human bacterial species—is quite similar to that of GF mice, which have no viable gut bacteria at all.

A Rat Microbiota Does Not Increase Intestinal T Cell Numbers in GF Mice

To further evaluate whether intestinal immune maturation depends on host-specific bacterial species, we colonized GF mice with a second foreign microbiota: that from rat gut. Different diets can drastically alter microbial community structure (Turnbaugh et al., 2009b); because mice and rats are fed a similar rodent diet, such effects are minimized in this model. GF mice underwent oral gavage with feces from Sprague-Dawley rats and were bred in a gnotobiotic isolator to obtain offspring colonized at birth with rat microbiota (RMb). Like the HMb, the RMb was not as effective as the MMb in expanding T cell numbers in all four gut compartments examined (Figure 3G). In

(B) Relative abundance of major bacterial phyla in the gut microbiota from MMb and HMb mice is shown. P0, parents; F1, first-generation offspring; F2, second-generation offspring. Each bar represents an individual mouse. Apparent differences in the Firmicutes-to-Bacteroidetes ratio between inoculum samples and recipients may have resulted from the observed differential DNA extraction performances of fecal suspensions (high water content) and fecal pellets (low water content).

(C–E) Detailed relative abundance of bacterial taxa in the three most abundant major phyla is presented.

(F) Number (percentage) of shared OTUs in each major bacterial phylum in MMb and HMb fecal pellets is demonstrated. See also Figures S1D and S1E.

(G and H) Gut microbial communities from individual mice, clustered according to principal coordinates analysis of unweighted UniFrac distances, is illustrated. Percentages of variation explained by plotted principal coordinates P1 and P2 are indicated on the x and y axes, respectively.

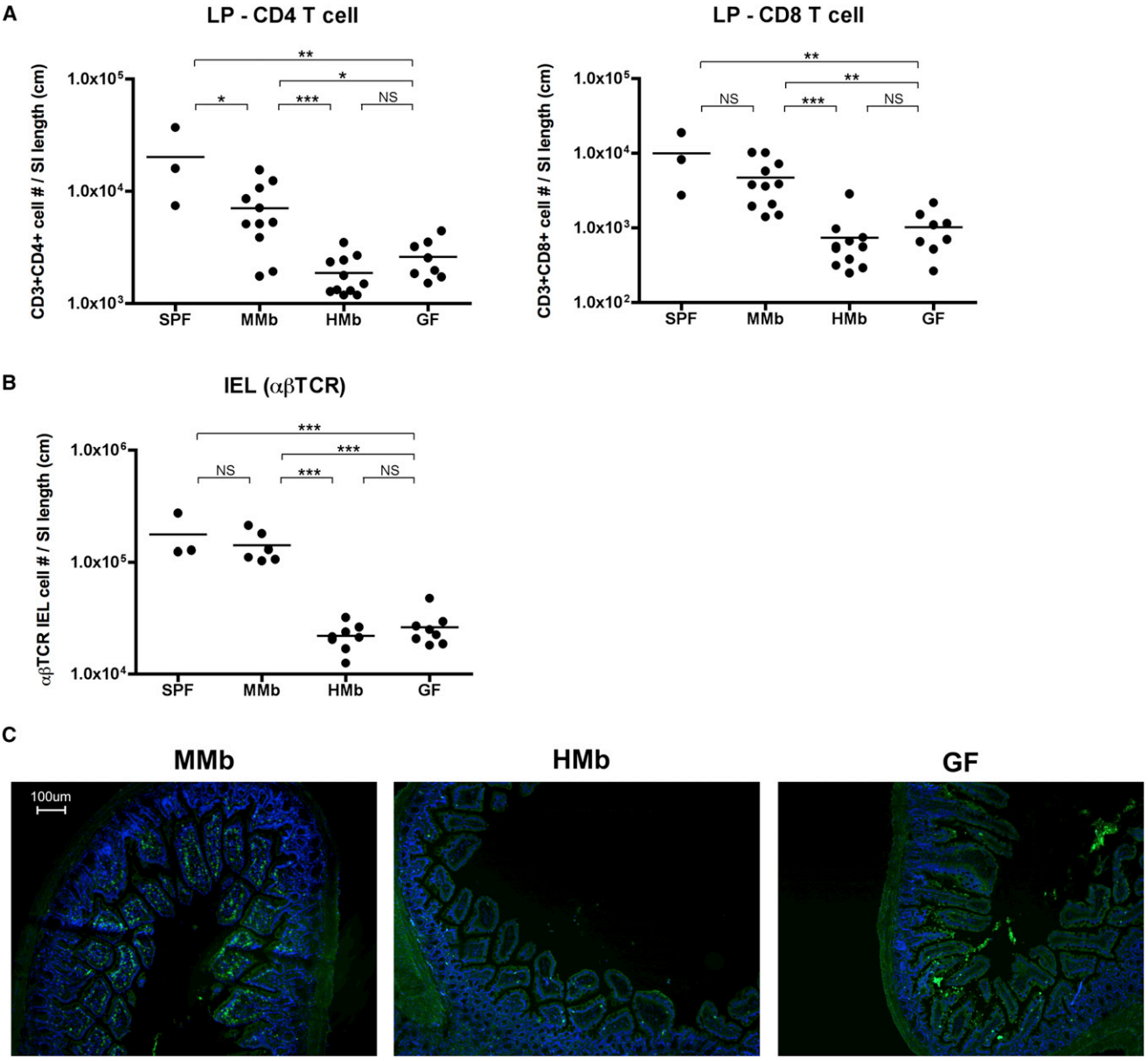

Figure 2. MMb Mice Have More Small Intestinal T Cells Than Do HMb Mice

(A and B) IELs were extracted from the small intestine; the remaining LP tissue was digested. Absolute numbers of $CD3^+CD103^+TCR\beta^+$ among IELs (B) and $CD3^+CD4^+$ and $CD3^+CD8^+$ cells from LP (A) were quantitated by flow cytometry and normalized to small intestine length. SPF and GF SW mice were age matched. See also Figures S2A and S2B. *$p < 0.05$, **$p < 0.01$, ***$p < 0.001$. NS, not significant.

(C) Sections of small intestine were stained with FITC-conjugated antibody to CD3 (green) and counterstained with DAPI (blue).

other words, neither the microbiota from 12 human donors nor that from rat donors restored T cell numbers in the mouse gut. Therefore, certain host-specific bacterial species appear to be required for intestinal immune maturation.

T Cell Proliferation Plays a Role in Expansion of Small Intestinal T Cells and Depends on a Host-Specific Microbiota

Recruitment of $CD4^+$ and $CD8\alpha\beta^+$ T cells to the mucosa reportedly is initiated through antigen uptake by antigen-presenting cells (APCs) in intestinal tissue followed by further priming and activation of naive lymphocytes by antigen-loaded APCs in secondary lymphoid organs such as PPs and MLNs. Primed lymphocytes expressing $\alpha4\beta7$ and CCR9 in secondary gut lymphoid organs enter the bloodstream and ultimately exit into gut tissue through vessels in the small intestinal LP where MAdCAM and CCL25—ligands of $\alpha4\beta7$ and CCR9, respectively—are expressed (Mowat, 2003). Because we found low numbers of T cells in both small intestinal tissue (IEL compartment, LP) and secondary lymphoid organs (PPs, MLNs) of

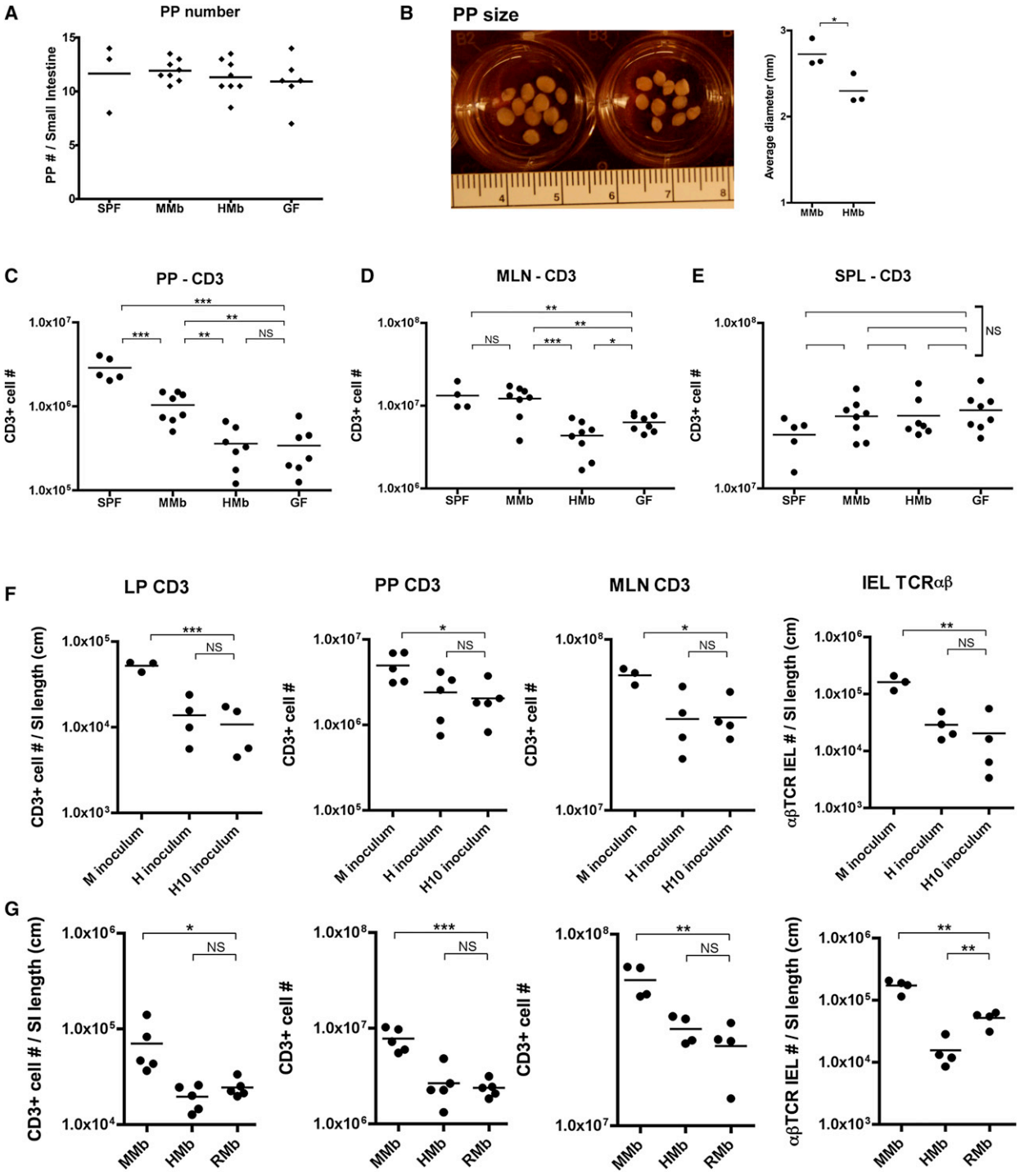

Figure 3. The MMb, but Not the HMb or RMb, Expands T Cell Populations in Small Intestinal Tissue and Secondary Gut Lymphoid Organs

(A–C) PP number (A) and average PP size (B) per small intestine were compared. PPs were mashed, stained for CD3, and subjected to flow cytometry (C). See also Figures S3A and S3B.

(D and E) Total T cell numbers in MLNs (D) and spleen (E) are shown. See also Figures S3C–S3G.

(F) GF mice (3–4 weeks old) were orally gavaged with the original mouse (M) or human (H) inoculum or with feces pooled from ten additional human donors (H10 inoculum). T cell numbers were measured after 4 weeks of colonization.

(G) GF mice were orally gavaged with Sprague-Dawley rat feces and bred in vinyl isolators to obtain RMb offspring. T cell numbers in age-matched MMb, HMb, and RMb offspring were compared.

*$p < 0.05$, **$p < 0.01$, ***$p < 0.001$. NS, not significant.

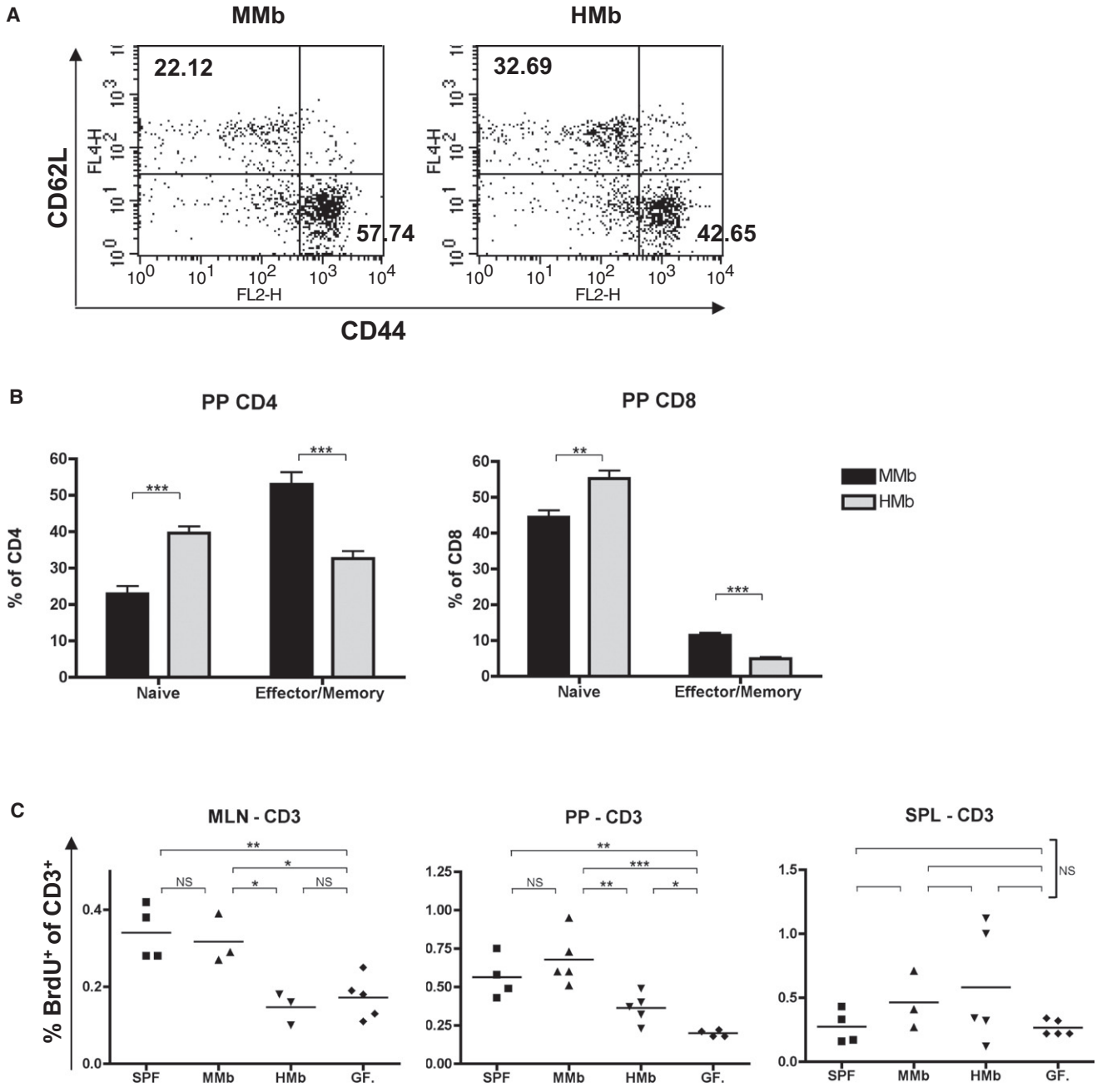

Figure 4. Host-Specific Gut Microbiota Induction of T Cell Proliferation in Secondary Gut Lymphoid Organs Leads to Expansion of Small Intestinal T Cells

(A) Representative flow cytometry plots of $CD44^{hi}CD62L^{lo}$ (effector/memory) and $CD44^{lo}CD62L^{hi}$ (naive) expression on $CD3^{+}CD4^{+}$ T cells in PPs of MMb and HMb offspring are presented. Numbers indicate cell percentages in the quadrant.

(B) Combined data for PP $CD3^{+}CD4^{+}$ and $CD3^{+}CD8^{+}$ cells (n = 7) are illustrated.

(C) Mice injected with BrdU were sacrificed 2 hr later. $CD3^{+}$ T cells were stained with FITC-conjugated antibody to BrdU for detection of proliferating cells. See also Figures S4A–S4C.

*p < 0.05, **p < 0.01, ***p < 0.001. NS, not significant.

HMb mice, we wondered whether there was a deficiency in T cell activation in the PPs and MLNs of these mice.

When we compared $CD4^{+}$ T cells in PPs of HMb and MMb mice, we found a lower frequency of effector/memory cells ($CD44^{hi}CD62L^{lo}$) but a higher frequency of naive T cells ($CD44^{lo}CD62L^{hi}$) in HMb mice. Analysis of $CD8^{+}$ T cells in PPs yielded similar results (Figures 4A and 4B). T cell activation in secondary lymphoid organs can also be assessed by

measurement of T cell proliferation frequencies. Mice were injected with bromodeoxyuridine (BrdU), which is incorporated into proliferating cells; the animals were sacrificed 2 hr later, and T cell proliferation frequencies were measured. This time point was chosen to exclude the possibility that BrdU-positive cells were migrating from a distant organ to MLNs and PPs (Rakoff-Nahoum et al., 2004). No differences were evident in the frequency of BrdU-positive T cells in the spleen and peripheral lymph nodes of MMb and HMb mice. However, the frequency of BrdU-positive $CD3^+$ cells in PPs and MLNs was significantly higher in MMb offspring than in HMb offspring. Comparable differences were found in both $CD4^+$ and $CD8^+$ T cell subsets (Figures 4C and S4A). These differences in T cell proliferation were also observed between SPF and GF mice (Figure 4C). Differences in T cell proliferation were confirmed by staining with Ki-67, an antigen associated with proliferating cells (Figure S4B). BrdU-positive T cells in PPs and MLNs, but not in spleen, expressed high and comparable levels of the small-intestine-homing markers CCR9 and $\alpha4\beta7$ in both MMb and HMb mice (Figure S4C). This result suggested that proliferating T cells in secondary lymphoid organs (PPs, MLNs) are imprinted to populate small intestinal tissue (IELs, LP). These data are consistent with the hypothesis that lower T cell proliferation in secondary lymphoid organs of HMb mice can contribute to T cell deficiency throughout the small intestine. Intriguingly, T cell proliferation in secondary lymphoid organs depended on colonization with host-specific bacterial species in the intestinal lumen.

It is certainly possible that immunologic mechanisms besides T cell proliferation contribute to the deficiency in T cell numbers in HMb mice. In PPs, but not in MLNs, we observed a higher rate of T cell apoptosis in HMb and GF mice than in MMb mice; thus, T cell death may play a role in diminishing T cell numbers in some intestinal compartments (Figure S4D). We also addressed whether T cells in HMb mice are deficient in homing to the intestine. DCs from PPs imprint CCR9 and $\alpha4\beta7$ on T cells upon activation (Mora et al., 2003), with consequent homing of activated T cells to intestinal tissue where their respective ligands are expressed. MMb and HMb offspring DCs (MLNs, PPs) similarly upregulated CCR9 and $\alpha4\beta7$ expression on T cells (Figure S4E). There was no significant difference in MMb and HMb intestinal recruitment of gut-homing T cells (Figure S4F). Analysis of small intestinal tissue consistently indicated no difference between MMb and HMb mice in expression of transcripts *MAdCAM* and *CCL25* (Figure S4G). Although other chemokines or adhesion molecules may contribute to differences in T cell numbers, these data suggest that T cell trafficking to the intestine via CCR9 and $\alpha4\beta7$ does not play a major role in differences between gut T cell counts in MMb and HMb mice.

HMb Mice Exhibit a Distinct Intestinal Gene Expression Profile

We addressed whether colonization with a foreign gut microbiota has effects beyond influencing T cell numbers, i.e., whether it also influences T cell phenotype. Using microarray analysis, we examined the transcriptional profiles of purified $CD4^+$ T cells from MMb, HMb, and GF mice. When we compared MMb and HMb mice with GF mice, we found that few genes were differentially expressed in $CD4^+$ T cells from spleen and MLNs, whereas differences were much more extensive in the small intestinal LP (Figure 5A).

The changes induced in spleen and MLNs were largely shared in both locales, because many genes fall on the diagonal of the FoldChange/FoldChange plot in Figure 5B. In MLNs, we found a number of genes upregulated by both MMb and HMb, including T cell activation genes (*CD9*, *Bcl3*, and *Socs3*); conversely, heat shock transcripts (*Hspa1a*, *dnaja1*, *dnajb1*, *dnajb4*), which are generally expressed at low levels in normal nonstressed cells (Glover and Lindquist, 1998), exhibited greater expression in MLN $CD4^+$ T cells from GF mice than in those from MMb and HMb mice—perhaps a reflection of the abnormal physiological conditions in GF mice (Figure 5B). In the spleen, some genes (e.g., *CD9* and heat shock transcripts) were expressed in a pattern similar to that in MLNs (Figure S5A).

In the small intestinal LP, where transcriptional changes were more extensive, the effects were more profound in MMb mice than in HMb mice. Many of the changes affected the same transcripts (Figure 5C) but were far more extensive in $CD4^+$ T cells from the LP of MMb mice, as denoted by the off-diagonal disposition of most transcripts. Most of these induction events affected cytokine genes, particularly those of the T_H17 family, i.e., interleukin-17a (*Il17a*), *Il17f*, and *Il22*. The induction of these cytokine genes was stronger in MMb mice (30- to 80-fold) than in HMb mice (2- to 5-fold). Closer examination of cytokine transcripts (Figure 5D) showed that $CD4^+$ T cells from the LP indeed expressed higher levels of T_H17 transcripts in MMb mice, whereas those from the LP of HMb mice expressed higher levels of *Il4*—indicative of stronger T_H2-type differentiation. Interferon γ (*Ifn*γ), the hallmark of T_H1 cells, was induced to the same levels in MMb and HMb mice. *Rorc* and *Rora*—transcription factors that control T_H17 cell differentiation (Ivanov et al., 2006; Yang et al., 2008)—were more strongly induced in MMb mice than in HMb or GF mice. Furthermore, *Gata3*—the transcription factor that controls T_H2-type differentiation—was detected at higher levels in HMb and GF mice than in MMb mice (Figures S5B and S5C). Thus, colonization with different bacterial species resulted in reciprocal bias in T cell effector phenotypes. These analyses indicated that host specificity of bacteria drastically affects both T cell numbers and phenotypes in the small intestinal LP.

In addition to isolated T cells, we studied gene transcription profiles in ileal tissue. Ilea from MMb mice exhibited enhanced expression of a collection of B cell-specific genes over levels in HMb and GF ilea (Figure S5D). Histologic examination also showed more intestinal IgA^+ cells in MMb mice than in HMb mice; in addition to T cell deficiencies, the HMb mouse gut has deficiencies in B cell maturation (Figure S5E). Microarray analysis of ileal tissue showed that certain chemokines (*CCL20*, *CCL28*, *CXCL9*) critical for T cell and DC chemotaxis and activation in the gut (Kunkel et al., 2003) are more strongly induced in MMb mice than in HMb or GF mice. These chemokines are expressed by the epithelium, at the interface between gut bacteria and host (Figure S5F). The host epithelium may be more apt to sense host-specific than foreign commensals.

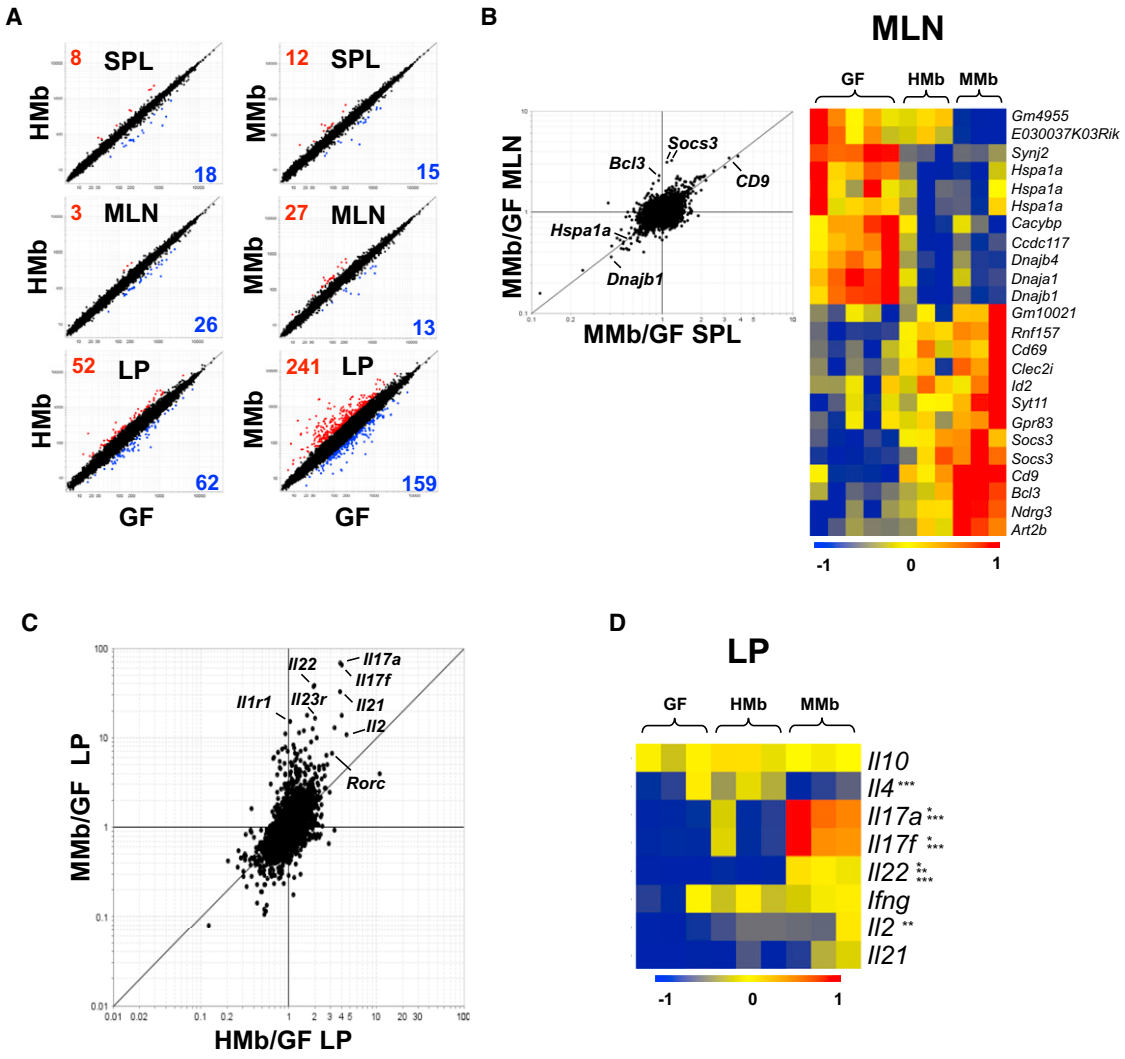

Figure 5. Distinct Gene Expression Profile in Small Intestinal T Cells from HMb Mice

(A) Microarray analysis comparing $CD4^+$ T cell gene expression in GF mice with that in HMb mice (left) and MMb mice (right) is demonstrated. $CD4^+$ T cells were sorted from spleen (SPL), MLNs, and small intestinal LP. Data are mean values from three to five independent experiments. Numbers indicate genes showing a $\geq$2-fold difference in expression between groups; red numbers indicate overexpression and blue numbers underexpression.

(B) Fold change versus fold-change analysis compares MMb mice with GF mice in terms of gene expression in $CD4^+$ T cells sorted from MLNs (y axis) and spleen (x axis) (left). A heatmap (right) shows differentially expressed genes in $CD4^+$ T cells sorted from the MLN. Some genes (*Hspa1a*, *Socs3*) were detected with multiple probes. Genes with the highest and lowest transcript levels are red and blue, respectively. See also Figure S5A.

(C) Fold change versus fold-change analysis compares gene expression in $CD4^+$ T cells sorted from small intestinal LP of GF mice versus MMb mice (y axis) or HMb mice (x axis).

(D) Heatmap shows differential cytokine expression in $CD4^+$ T cells from small intestinal LP. Data are from three independent experiments. See also Figures S5B–S5F. *p < 0.05, MMb versus GF; **p < 0.05, HMb versus GF; ***p < 0.05, HMb versus MMb.

Segmented Filamentous Bacteria Only Partially Expand Mouse Intestinal T Cell Numbers

Strong induction of T_H17 cell-associated gene transcripts in MMb mice led us to assess the presence of segmented filamentous bacteria (SFB) in our mouse colony. SFB are commensal gut bacteria found in mammals such as mice, rats, and chickens (Snel et al., 1995) and are potent inducers of T_H17 cells (Gaboriau-Routhiau et al., 2009; Ivanov et al., 2009). Genome sequence analysis showed that SFB lack virulence-related genes and may depend largely on the host for amino acids and essential nutrients (Prakash et al., 2011; Sczesnak et al., 2011). In an SFB-specific qPCR assay for 16S rDNA in multiple mammalian species, we found that all MMb mice (and the MMb inoculum) carried SFB DNA. In contrast, all HMb mice (and the HMb inoculum) were negative for SFB (Figure 6A). Although there is no DNA sequence-based evidence for SFB in humans, these bacteria are members of the highly host-specific phylum Firmicutes (Figures 1F and S1E), and other Firmicutes may play a role in humans similar to that played by SFB in mice.

Besides inducing T_H17 cells, SFB increase IEL numbers (Umesaki et al., 1999). We tested whether SFB played a role in expansion of IELs in our MMb colony. Although SFB-monocolonized mice had extremely high SFB numbers (Figure 6A), their absolute αβTCR IEL numbers were higher than those in GF mice but significantly lower than those in MMb mice—differences suggesting that SFB alone only partially restored the αβTCR IEL population (Figure 6B). SFB fully expanded absolute numbers of CD8αα-αβTCR IELs—a unique self-reactive population that requires exposure to self-agonists for selection in the thymus (Leishman et al., 2002)—but only partially expanded the CD8αβ-αβTCR IELs, which is generated mostly in secondary lymphoid organs and is primed against nonself-antigens (Figures S6A–S6C). Likewise, in other sites (e.g., PPs and LP), SFB monocolonization partially increased $CD4^+$ and $CD8^+$ T cell numbers but did not fully restore T cell numbers to levels in MMb mice (Figures 6B and S6D). To examine whether the transfer of SFB or microbes from MMb into HMb mice could fully rescue T cell numbers, we separately cohoused HMb mice with either MMb mice or SFB-monocolonized mice. Despite comparable levels of SFB transfer into the two groups (Figure S6E), HMb mice cohoused with MMb mice had more T cells in the IEL compartment, PPs, and LP than HMb mice cohoused with SFB-monocolonized mice (Figures 6C, S6C, and S6D). In addition to SFB, other critical mouse bacterial species may induce immune maturation in mouse gut.

In PPs, SFB appear to play a more prominent role in expanding $CD4^+$ T cells than $CD8^+$ T cells (Figure 6B). Inflammatory $CD4^+$ $RORgt^+$ T cells as well as anti-inflammatory $CD4^+Foxp3^+$ T cells are critical in maintaining homeostasis in the gut (Hand and Belkaid, 2010). In contrast to MMb, SFB monocolonization only partially expanded $CD4^+RORgt^+$ T cells (Figures 6D and S6F) and failed to increase $CD4^+Foxp3^+$ cell numbers in PPs (Figure 6E). The increased percentage of $CD4^+Foxp3^+$ cells in PPs of HMb and GF mice (Figure S6G) was due not to an increase in absolute $CD4^+Foxp3^+$ cell numbers but rather to a prominent lack of $CD4^+RORgt^+$ cells. The failure of SFB and HMb to expand $CD4^+Foxp3^+$ populations in PPs (Figure 6E) suggests that mouse-specific bacterial species besides SFB may induce Foxp3 expression.

Rats carry SFB similar in morphology and 16S rRNA sequence to mouse-specific SFB (Klaasen et al., 1993; Snel et al., 1995). To determine whether rat SFB can colonize mice, we sought rat SFB in RMb mice. Fecal pellets from Sprague-Dawley rats that were used to prepare the RMb inoculum were positive for SFB by qPCR (Figure 6F). Using Gram's stain, we observed organisms with long filamentous structures suggestive of SFB in Sprague-Dawley rat fecal pellets (Figure 6G). However, SFB were not detected in any samples from RMb mice—not even from the parent generation—as soon as 3 days after gavage of the RMb inoculum (Figure 6F).

We conclude that SFB in the mouse gut microbiota play a role in expanding intestinal T cell numbers but do not act alone. We found no sequence-based evidence for SFB in HMb inocula or in our HMb mouse colony. When introduced as part of a complex microbiota, rat SFB did not colonize mice. Therefore, SFB exemplify a host-specific Firmicute lineage. These observations support the hypothesis that the mammalian gut selects for host-specific bacterial species, an effect that in turn strengthens the intestinal immune system.

HMb Mice Are More Susceptible Than MMb Mice to *Salmonella* Infection

An intact gut microbiota is critical for mucosal protection from bacterial invasion and disease (Ferreira et al., 2011). Furthermore, a high total gut bacterial load alone is insufficient to protect against infection; rather, certain bacterial species correlate with protection (Croswell et al., 2009). Therefore, we orally infected MMb and HMb mice with *Salmonella enterica* serovar Typhimurium, a zoonotic and clinically relevant pathogen that can be acquired via contaminated food. MMb mice had a significantly lower *Salmonella* load in feces and less dissemination to the spleen. Interestingly, SFB-monocolonized mice were colonized with high levels of *Salmonella* similar to GF mice (Figures 7A and 7B). At 4 days after infection, MMb mouse ceca appeared healthy on histology, whereas ceca of HMb, SFB, and GF mice had severe gross pathological changes characterized by thickening of the cecal wall, inflammation, and edema (Figure 7C). Our conclusion that a host-specific microbiota is most effective in defense against an important gastrointestinal disease further supports the hypothesis that hosts may have coevolved with a beneficial host-specific microbiota.

DISCUSSION

Host-Specific Bacteria Influence Intestinal Immune Maturation

It was reported that short-term colonization of adult GF mice with a human gut microbiota results in a low αβTCR/γδTCR ratio among IELs (Imaoka et al., 2004). Another study documented a predominance of downregulated transcripts in the ilea of mice given human feces (Gaboriau-Routhiau et al., 2009). However, these reports did not clarify whether such phenotypes were due to stalled intestinal immune maturation, an aberrant local effect, or failure to colonize at an early enough age. We analyzed absolute T cell numbers in intestinal compartments of mice naturally colonized with an HMb at birth. Technical advances in high-throughput sequencing permitted deep sampling of 16S rRNA genes and detailed comparison of MMb and HMb after introduction into GF mice—analyses not feasible in the two previous studies.

MMb and HMb mouse gut microbiotas are similar in relative abundances of the major bacterial phyla but have substantial differences at the OTU level, particularly among Firmicutes. Colonization with HMb results in an immature adaptive and innate intestinal immune system, most notably in the small intestine. HMb mice have low numbers of intestinal T cells (partly because of less T cell activation/proliferation) and DCs. HMb mice intestine also displays low-level expression of *RegIIIγ*, IgA, and various chemokines (*CCL20*, *CCL28*, *CXCL9*) (Figure S7; Table S3). The lack of difference between MMb and HMb mice in large intestinal LP $CD3^+$ and αβTCR IEL numbers suggests that the microbiota regulates the small and large intestinal immune compartments via distinct mechanisms.

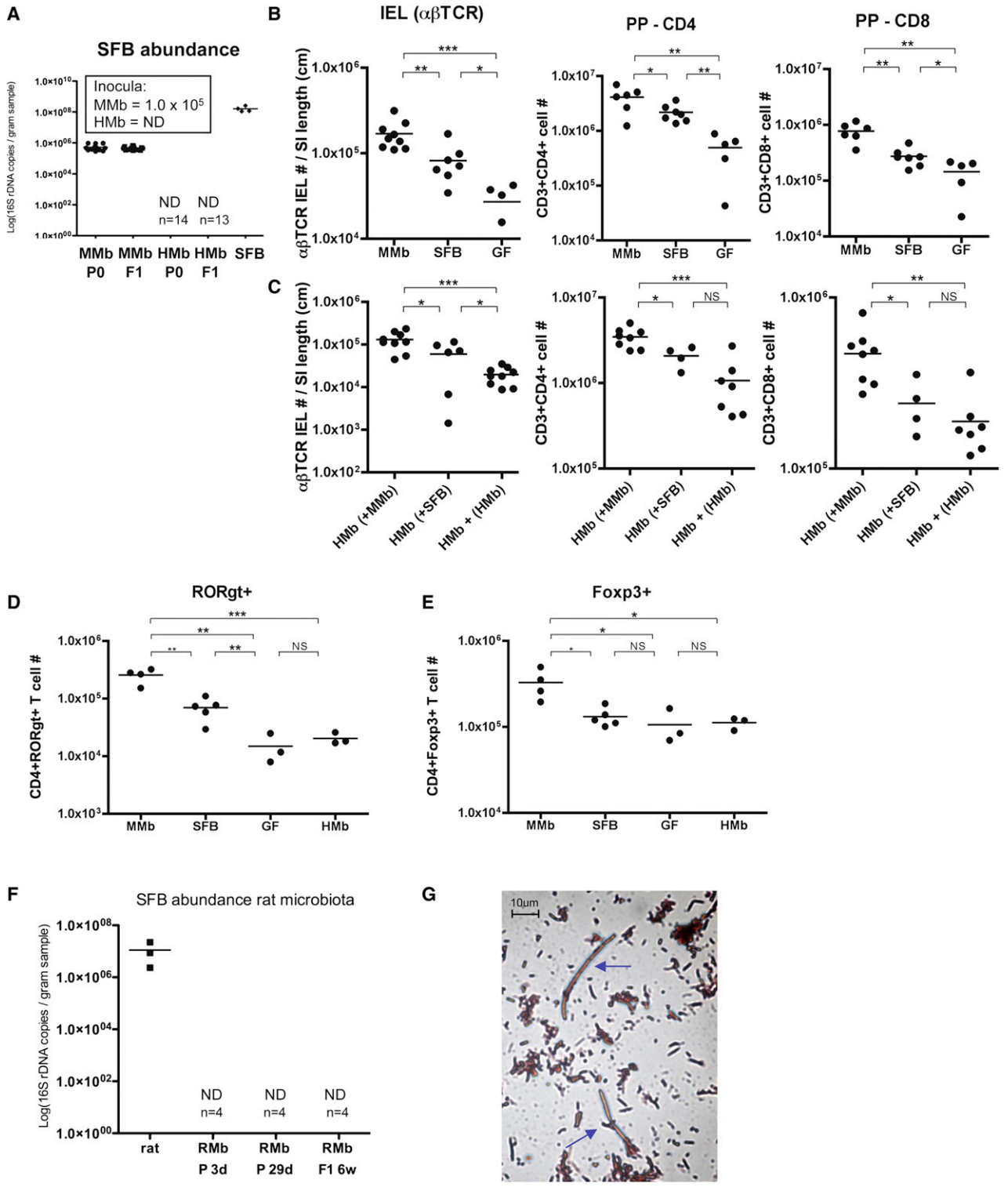

Figure 6. SFB Play a Role in Rescuing Intestinal T Cell Numbers and Exhibit Host Specificity

(A) Abundance of SFB in MMb, HMb, and SFB-monocolonized mice, measured as SFB-specific 16S rDNA copy numbers by qPCR analysis of fecal pellets, is shown. Inset values indicate number of SFB 16S rDNA copies/ml in inocula. ND, not detected.

(B and C) Absolute T cell numbers in IEL ($CD3^+CD103^+TCR\beta^+$) and PP ($CD3^+CD4^+$ and $CD3^+CD8^+$) compartments of MMb, SFB-monocolonized, and GF mice (B) and HMb mice cohoused with MMb or SFB-monocolonized mice for 4 weeks (C) are presented. In (C), as a negative control, HMb mice were cohoused with HMb mice. See also Figures S6A–S6E.

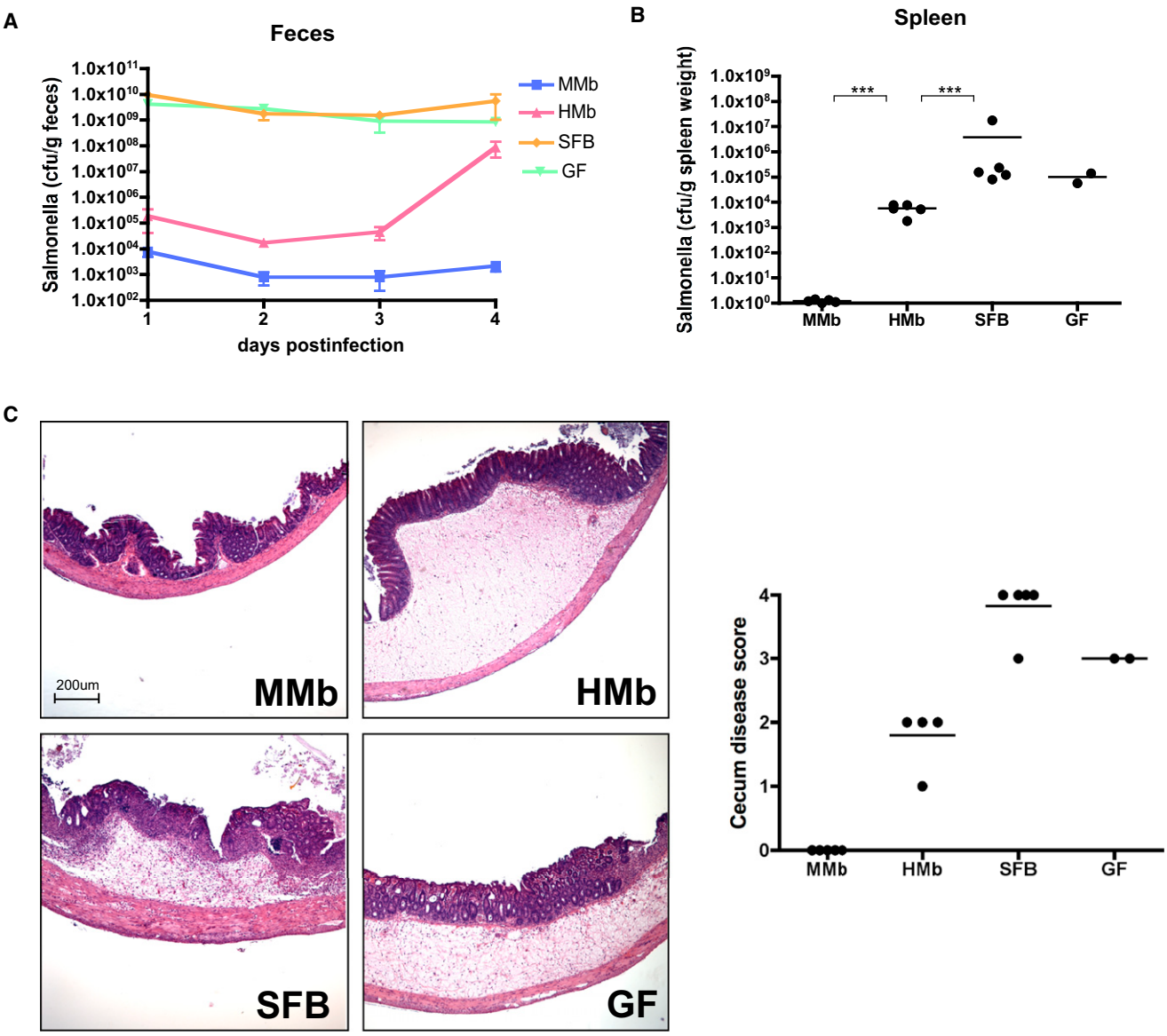

Figure 7. MMb Confers Better Protection against *Salmonella enterica* Serovar Typhimurium Than HMb

(A–C) Mice colonized with different microbiotas were orally gavaged with ~1 × 10^7 salmonellae; the *Salmonella* load in fecal pellets was measured daily (A). Mice were sacrificed on day 4 after infection, and the *Salmonella* load in the spleen was measured (B). Cecal sections were stained with hematoxylin and eosin, and disease was scored (C). ***p < 0.001.

Mouse SFB (Firmicutes), but not rat SFB, established colonization in the mouse gut. Rat SFB may not have adhered efficiently to mouse epithelium. In addition, there may exist a host-specific microbial ecology that supports prolonged SFB colonization, especially because SFB may function as an adjuvant for the immunostimulatory functions of other resident gut microbes (Chung and Kasper, 2010). The exclusive partnership of SFB with the host is a proof of concept that the mammalian

(D and E) Number of $CD3^+CD4^+$ T cells in PPs expressing $RORgt^+$ (D) and $Foxp3^+$ (E), as derived by intracellular staining and flow cytometry, is illustrated. See also Figures S6F–S6G.

(F) Abundance of SFB in fecal samples from Sprague-Dawley rats and RMb-colonized mice, measured as SFB-specific 16S rDNA copy numbers by qPCR, is shown. Fecal pellets from RMb parents were collected on postgavage days 3 (RMb P 3d) and 29 (RMb P 29d); those from RMb offspring were collected at 6 weeks of age (RMb F1 6w). ND, not detected.

(G) Gram-stained Sprague-Dawley rat fecal pellets resuspended in PBS are illustrated. Blue arrows indicate bacteria with long filamentous structures representative of SFB.

*p < 0.05, **p < 0.01, ***p < 0.001. NS, not significant.

gut selects for host-specific bacterial species that enhance host immunity. SFB alone partially restored gut T cell numbers but were not fully protective against *Salmonella* infection—results suggesting that SFB are one but not the only MMb component responsible for immune maturation and protection against infection.

There is redundancy in the gut microbiota in facilitating certain host metabolic functions; i.e., individual HMbs can vary at the bacterial species level but nonetheless share functional genes (Turnbaugh et al., 2009a). A study of GF zebrafish colonized with a MMb showed that a foreign microbiota can partially restore transcription of host genes involved in nutrient absorption and metabolism (Rawls et al., 2006). Despite such bacterial species-level redundancy in stimulating host metabolic functions, our HMb mouse studies demonstrate that the host intestinal immunity maturation depends on a strict set of host-specific bacterial species.

Mechanisms of Intestinal Immune Maturation

We show that host-specific bacterial species induce expansion of intestinal T cells by stimulating T cell activation/proliferation in secondary gut lymphoid organs (PPs and MLNs), with consequent effects on downstream T cell numbers in intestinal tissue (IELs and LP) (Figure S7; Table S3). Many questions remain about the causes of the differences in T cell proliferation. Reduced numbers of DCs in the PPs and MLNs of HMb mice may have caused lower T cell proliferation rates. The MMb, but not the HMb, may induce a cytokine or chemokine milieu effective in activating and recruiting APCs to stimulate downstream T cell proliferation.

We believe that the higher rate of T cell proliferation in MMb mice is predominantly antigen driven. Although the small intestinal epithelium is protected by mucus and antimicrobial peptides (Johansson and Hansson, 2011), certain host-specific microbes may reside near the epithelium and induce antigen uptake from the lumen by stimulating APCs or by modulating the gut epithelial barrier. Compared to HMb, MMb may be more efficient at penetrating the mouse mucus layer or evading certain mouse antimicrobial peptides. Alternatively, certain host-specific microbiotas may regulate epithelial sensitivity in recognizing microbe-associated molecular patterns (MAMPs) through pattern recognition receptors (Eberl and Boneca, 2010). An understanding of these mutually nonexclusive mechanisms potentially employed by the host microbiota could guide efforts to modulate gut immunity in order to improve host health.

The Gut Microbiota, Host Health, and Evolution

HMb mice are more susceptible to *Salmonella* infection than MMb mice. Because adaptive immunity (T cells) and innate immunity (antimicrobial peptides, DCs) are both critical for defense against *Salmonella* infection (Salazar-Gonzalez et al., 2006; Vaishnava et al., 2008), the absence of an intact immune system in HMb mice likely played a role in susceptibility to *Salmonella* infection. In addition, MMb might have been more effective than HMb in physically inhibiting enteropathogen adherence (Heczko et al., 2000). Infectious disease epidemics are among the most powerful selective forces acting on hosts and microbes. We speculate that, throughout evolution, hosts coexisting with bacteria that were well adapted to the host gut environment and capable of enhancing host health survived particular epidemics. Selection against hosts lacking such bacterial species may have promoted the survival and enrichment of beneficial host-specific bacteria.

The Human Microbiome

Metagenomic analysis of the gut microbiota of 124 Europeans suggested that humans share many bacterial species (Qin et al., 2010). Widely shared human-specific bacterial species may not predominate in the gut microbiota, and their prevalence may vary substantially with the individual and perhaps with age. Nonetheless, these microorganisms may be potent stimulators of host immunity. Surveys for SFB-like microbes residing closer to the gut epithelium or for *Alcaligenes* species within PPs (Obata et al., 2010) may help identify immunomodulatory human microbes.

HMb-colonized mice have been proposed as a useful tool to study human metabolism and disease (Turnbaugh et al., 2009b). Some, but not all, human microbes may be immunostimulatory in a GF mouse monocolonization model. Amplification of one specific microbe may enhance the likelihood of observing a function of that microbe, which otherwise would exert no observable function in a mouse colonized with a complex HMb. For example, the immunomodulatory effects of the human microbe *Bacteroides fragilis*, which cannot readily colonize the conventionally colonized mouse intestine, were first reported in *B. fragilis*-monocolonized mice (Mazmanian et al., 2005). Therefore, such GF mouse monocolonization models should be taken into consideration in defining the function of widely shared human microbes.

Revisiting the Hygiene Hypothesis

The revised hygiene hypothesis proposes that exposure to immunomodulatory gut commensals can provide protection from autoimmune diseases (Wills-Karp et al., 2001). Our immunologic analysis of mice colonized with human gut bacteria suggests that exposure to just any gut commensal microbe or its MAMPs (e.g., lipopolysaccharide, cell wall components) is insufficient to induce intestinal immune maturation. Our study rather suggests that only certain host-specific commensals give rise to a mature intestinal immune system. Because the intestinal microbiota can regulate immune responses outside the gut (Wen et al., 2008; Wu et al., 2010), the absence of the "right" gut microbes may conceivably shift the balance toward disease in individuals genetically predisposed to autoimmune diseases.

Heavy processing of food, frequent treatment with antibiotics, and advances in hygiene in industrialized countries may have reduced the stability and transfer of host microbes promoting health. Furthermore, because advances in medicine and technology provide alternative ways to fight disease, humans may be becoming less dependent on their coevolved gut microbiota for health and survival. The current prevalence of autoimmune diseases may be, at least in part, the consequence of increasing vulnerability of the coevolved human-microbe relationship.

EXPERIMENTAL PROCEDURES

Mice and Colonization

SPF and GF SW mice (Taconic Farms) and Sprague-Dawley rats (Harlan) were used. Cecal/fecal contents from ten SPF SW mice served as the MMb inoculum, fresh human feces from two healthy Caucasian adults (one male, one female) as the HMb inoculum, and fecal pellets from four Sprague-Dawley rats as the RMb inoculum. The human donors had not taken antibiotics for 1 year. Fecal contents were diluted (10^{-1}) in prereduced peptone yeast glucose, snap frozen in liquid nitrogen, and stored at −80°C. SW GF mice (3–4 weeks old) received inocula by oral gavage and were then placed in sterile vinyl isolators. Mice were bred in the isolators to obtain offspring and were maintained on an autoclaved NIH-31M rodent diet (Taconic Farms). All procedures with animals were performed according to HMS Office for Research Subject Protection guidelines. Human samples were collected according to Partners Human Research Committee guidelines.

Microbiota Analysis

16S rDNA was amplified from fecal pellets and inoculum samples and subjected to GS-FLX titanium multiplex pyrosequencing (Roche). Reads were filtered and quality trimmed. Phylogenetic assignments were made by clustering reads against a high-quality seed library with Uclust. UniFrac distances were calculated and principal coordinates analyses performed with QIIME software. See Extended Experimental Procedures for detailed analysis and references.

Cell Isolation and Flow Cytometry

PPs were excised from the small intestine, and the remaining tissue was incubated with 1 mM DTT/1 mM EDTA/3% FBS/PBS (30 min, 37°C) for IEL extraction. Residual intestinal tissue was digested in 5% FBS RPMI with 0.15% collagenase II (275 U/mg)/0.05% dispase (1.1 U/mg) (Invitrogen) for 1 hr at 37°C. IELs and LP cells were filtered to minimize mucus contamination. Single-cell suspensions of MLNs, PPs, spleen, and peripheral lymph nodes were prepared by mashing in a cell strainer (70 μm). Cells were stained with fluorophore-conjugated mouse antibodies, and flow cytometry was performed with Fluorospheres/FLOW-COUNT (Beckman Coulter) beads.

Microarray Analysis

CD4+ T cells were isolated from spleen, MLNs, and small intestinal LP of 10- to 14-week-old mice (Feuerer et al., 2010). See also Extended Experimental Procedures.

Salmonella Infections

S. enterica serovar Typhimurium strain SL1344 was grown at 37°C in Luria-Bertani (LB)/streptomycin (200 μg/ml). Mice (8–10 weeks old) were orally gavaged with ~5×10^7 cfu. Fecal samples and spleens were homogenized in PBS and plated on LB/streptomycin (200 μg/ml) agar. Ceca were fixed in Bouin's solution and stained with hematoxylin and eosin. Slides were scored for inflammation, ulceration, and edema as follows: 0, no disease; 1, mild; 2, moderate; 3, severe; 4, very severe.

Statistical Analysis

All p values were calculated by unpaired/two-tailed t test. In dot plots, each data point represents an individual mouse, and horizontal bars indicate the means.

ACCESSION NUMBERS

The 16S rDNA sequences have been deposited at GenBank under accession number SRA052958.

SUPPLEMENTAL INFORMATION

Supplemental Information includes Extended Experimental Procedures, seven figures, and four tables and can be found with this article online at doi:10.1016/j.cell.2012.04.037.

ACKNOWLEDGMENTS

We thank Shakir Edwards for gnotobiotic animal care, Julie B. McCoy for editing, Tom DiCesare for image design, Dr. Rod Bronson for pathology scoring, Jennifer Dinalo for ten human fecal samples, and Les Dethlefsen and Robert Edgar for helpful advice. This work was supported by a Senior Research Award from the Crohn's & Colitis Foundation of America (to D.L.K.), by the Juvenile Diabetes Research Foundation (to H.C.), by the Danish Council for Independent Research Natural Sciences (to S.J.P.), by National Institutes of Health Grant F32 AI091104 (to N.K.S.), and by Director's Pioneer Award DP1OD000964 (to D.A.R.). D.A.R. is supported by the Thomas C. and Joan M. Merigan Endowment at Stanford University.

Received: March 20, 2011
Revised: January 3, 2012
Accepted: April 7, 2012
Published: June 21, 2012

REFERENCES

Arumugam, M., Raes, J., Pelletier, E., Le Paslier, D., Yamada, T., Mende, D.R., Fernandes, G.R., Tap, J., Bruls, T., Batto, J.M., et al; MetaHIT Consortium. (2011). Enterotypes of the human gut microbiome. Nature *473*, 174–180.

Atarashi, K., Tanoue, T., Shima, T., Imaoka, A., Kuwahara, T., Momose, Y., Cheng, G., Yamasaki, S., Saito, T., Ohba, Y., et al. (2011). Induction of colonic regulatory T cells by indigenous *Clostridium* species. Science *331*, 337–341.

Bandeira, A., Mota-Santos, T., Itohara, S., Degermann, S., Heusser, C., Tonegawa, S., and Coutinho, A. (1990). Localization of gamma/delta T cells to the intestinal epithelium is independent of normal microbial colonization. J. Exp. Med. *172*, 239–244.

Chassin, C., Kocur, M., Pott, J., Duerr, C.U., Gütle, D., Lotz, M., and Hornef, M.W. (2010). miR-146a mediates protective innate immune tolerance in the neonate intestine. Cell Host Microbe *8*, 358–368.

Chung, H., and Kasper, D.L. (2010). Microbiota-stimulated immune mechanisms to maintain gut homeostasis. Curr. Opin. Immunol. *22*, 455–460.

Croswell, A., Amir, E., Teggatz, P., Barman, M., and Salzman, N.H. (2009). Prolonged impact of antibiotics on intestinal microbial ecology and susceptibility to enteric *Salmonella* infection. Infect. Immun. *77*, 2741–2753.

Dethlefsen, L., and Relman, D.A. (2011). Incomplete recovery and individualized responses of the human distal gut microbiota to repeated antibiotic perturbation. Proc. Natl. Acad. Sci. USA *108* (*Suppl 1*), 4554–4561.

Dethlefsen, L., McFall-Ngai, M., and Relman, D.A. (2007). An ecological and evolutionary perspective on human-microbe mutualism and disease. Nature *449*, 811–818.

Duan, J., Chung, H., Troy, E., and Kasper, D.L. (2010). Microbial colonization drives expansion of IL-1 receptor 1-expressing and IL-17-producing gamma/delta T cells. Cell Host Microbe *7*, 140–150.

Eberl, G., and Boneca, I.G. (2010). Bacteria and MAMP-induced morphogenesis of the immune system. Curr. Opin. Immunol. *22*, 448–454.

Eberl, G., Marmon, S., Sunshine, M.J., Rennert, P.D., Choi, Y., and Littman, D.R. (2004). An essential function for the nuclear receptor RORgamma(t) in the generation of fetal lymphoid tissue inducer cells. Nat. Immunol. *5*, 64–73.

Eckburg, P.B., Bik, E.M., Bernstein, C.N., Purdom, E., Dethlefsen, L., Sargent, M., Gill, S.R., Nelson, K.E., and Relman, D.A. (2005). Diversity of the human intestinal microbial flora. Science *308*, 1635–1638.

Ferreira, R.B., Gill, N., Willing, B.P., Antunes, L.C., Russell, S.L., Croxen, M.A., and Finlay, B.B. (2011). The intestinal microbiota plays a role in *Salmonella*-induced colitis independent of pathogen colonization. PLoS One *6*, e20338.

Feuerer, M., Hill, J.A., Kretschmer, K., von Boehmer, H., Mathis, D., and Benoist, C. (2010). Genomic definition of multiple ex vivo regulatory T cell subphenotypes. Proc. Natl. Acad. Sci. USA *107*, 5919–5924.

Gaboriau-Routhiau, V., Rakotobe, S., Lécuyer, E., Mulder, I., Lan, A., Bridonneau, C., Rochet, V., Pisi, A., De Paepe, M., Brandi, G., et al. (2009). The key

role of segmented filamentous bacteria in the coordinated maturation of gut helper T cell responses. Immunity *31*, 677–689.

Glover, J.R., and Lindquist, S. (1998). Hsp104, Hsp70, and Hsp40: a novel chaperone system that rescues previously aggregated proteins. Cell *94*, 73–82.

Hand, T., and Belkaid, Y. (2010). Microbial control of regulatory and effector T cell responses in the gut. Curr. Opin. Immunol. *22*, 63–72.

Heczko, U., Abe, A., and Finlay, B.B. (2000). Segmented filamentous bacteria prevent colonization of enteropathogenic *Escherichia coli* O103 in rabbits. J. Infect. Dis. *181*, 1027–1033.

Imaoka, A., Setoyama, H., Takagi, A., Matsumoto, S., and Umesaki, Y. (2004). Improvement of human faecal flora-associated mouse model for evaluation of the functional foods. J. Appl. Microbiol. *96*, 656–663.

Ivanov, I.I., McKenzie, B.S., Zhou, L., Tadokoro, C.E., Lepelley, A., Lafaille, J.J., Cua, D.J., and Littman, D.R. (2006). The orphan nuclear receptor RORgammat directs the differentiation program of proinflammatory IL-17+ T helper cells. Cell *126*, 1121–1133.

Ivanov, I.I., Atarashi, K., Manel, N., Brodie, E.L., Shima, T., Karaoz, U., Wei, D., Goldfarb, K.C., Santee, C.A., Lynch, S.V., et al. (2009). Induction of intestinal Th17 cells by segmented filamentous bacteria. Cell *139*, 485–498.

Johansson, M.E., and Hansson, G.C. (2011). Microbiology. Keeping bacteria at a distance. Science *334*, 182–183.

Kelsall, B.L., and Rescigno, M. (2004). Mucosal dendritic cells in immunity and inflammation. Nat. Immunol. *5*, 1091–1095.

Klaasen, H.L., Koopman, J.P., Van den Brink, M.E., Bakker, M.H., Poelma, F.G., and Beynen, A.C. (1993). Intestinal, segmented, filamentous bacteria in a wide range of vertebrate species. Lab. Anim. *27*, 141–150.

Koropatnick, T.A., Engle, J.T., Apicella, M.A., Stabb, E.V., Goldman, W.E., and McFall-Ngai, M.J. (2004). Microbial factor-mediated development in a host-bacterial mutualism. Science *306*, 1186–1188.

Kunkel, E.J., Campbell, D.J., and Butcher, E.C. (2003). Chemokines in lymphocyte trafficking and intestinal immunity. Microcirculation *10*, 313–323.

Leishman, A.J., Gapin, L., Capone, M., Palmer, E., MacDonald, H.R., Kronenberg, M., and Cheroutre, H. (2002). Precursors of functional MHC class I- or class II-restricted CD8alphaalpha(+) T cells are positively selected in the thymus by agonist self-peptides. Immunity *16*, 355–364.

Ley, R.E., Bäckhed, F., Turnbaugh, P., Lozupone, C.A., Knight, R.D., and Gordon, J.I. (2005). Obesity alters gut microbial ecology. Proc. Natl. Acad. Sci. USA *102*, 11070–11075.

Ley, R.E., Hamady, M., Lozupone, C., Turnbaugh, P.J., Ramey, R.R., Bircher, J.S., Schlegel, M.L., Tucker, T.A., Schrenzel, M.D., Knight, R., and Gordon, J.I. (2008a). Evolution of mammals and their gut microbes. Science *320*, 1647–1651.

Ley, R.E., Lozupone, C.A., Hamady, M., Knight, R., and Gordon, J.I. (2008b). Worlds within worlds: evolution of the vertebrate gut microbiota. Nat. Rev. Microbiol. *6*, 776–788.

Mazmanian, S.K., Liu, C.H., Tzianabos, A.O., and Kasper, D.L. (2005). An immunomodulatory molecule of symbiotic bacteria directs maturation of the host immune system. Cell *122*, 107–118.

Mazmanian, S.K., Round, J.L., and Kasper, D.L. (2008). A microbial symbiosis factor prevents intestinal inflammatory disease. Nature *453*, 620–625.

Mora, J.R., Bono, M.R., Manjunath, N., Weninger, W., Cavanagh, L.L., Rosemblatt, M., and Von Andrian, U.H. (2003). Selective imprinting of gut-homing T cells by Peyer's patch dendritic cells. Nature *424*, 88–93.

Mowat, A.M. (2003). Anatomical basis of tolerance and immunity to intestinal antigens. Nat. Rev. Immunol. *3*, 331–341.

Obata, T., Goto, Y., Kunisawa, J., Sato, S., Sakamoto, M., Setoyama, H., Matsuki, T., Nonaka, K., Shibata, N., Gohda, M., et al. (2010). Indigenous opportunistic bacteria inhabit mammalian gut-associated lymphoid tissues and share a mucosal antibody-mediated symbiosis. Proc. Natl. Acad. Sci. USA *107*, 7419–7424.

Ochman, H., Worobey, M., Kuo, C.H., Ndjango, J.B., Peeters, M., Hahn, B.H., and Hugenholtz, P. (2010). Evolutionary relationships of wild hominids recapitulated by gut microbial communities. PLoS Biol. *8*, e1000546.

Olszak, T., An, D., Zeissig, S., Vera, M.P., Richter, J., Franke, A., Glickman, J.N., Siebert, R., Baron, R.M., Kasper, D.L., et al. (2012). Microbial exposure during early life has persistent effects on natural killer T cell function. Science *336*, 489–493.

Pais, R., Lohs, C., Wu, Y., Wang, J., and Aksoy, S. (2008). The obligate mutualist *Wigglesworthia glossinidia* influences reproduction, digestion, and immunity processes of its host, the tsetse fly. Appl. Environ. Microbiol. *74*, 5965–5974.

Palmer, C., Bik, E.M., DiGiulio, D.B., Relman, D.A., and Brown, P.O. (2007). Development of the human infant intestinal microbiota. PLoS Biol. *5*, e177.

Prakash, T., Oshima, K., Morita, H., Fukuda, S., Imaoka, A., Kumar, N., Sharma, V.K., Kim, S.W., Takahashi, M., Saitou, N., et al. (2011). Complete genome sequences of rat and mouse segmented filamentous bacteria, a potent inducer of th17 cell differentiation. Cell Host Microbe *10*, 273–284.

Qin, J., Li, R., Raes, J., Arumugam, M., Burgdorf, K.S., Manichanh, C., Nielsen, T., Pons, N., Levenez, F., Yamada, T., et al; MetaHIT Consortium. (2010). A human gut microbial gene catalogue established by metagenomic sequencing. Nature *464*, 59–65.

Rakoff-Nahoum, S., Paglino, J., Eslami-Varzaneh, F., Edberg, S., and Medzhitov, R. (2004). Recognition of commensal microflora by toll-like receptors is required for intestinal homeostasis. Cell *118*, 229–241.

Rawls, J.F., Mahowald, M.A., Ley, R.E., and Gordon, J.I. (2006). Reciprocal gut microbiota transplants from zebrafish and mice to germ-free recipients reveal host habitat selection. Cell *127*, 423–433.

Round, J.L., and Mazmanian, S.K. (2009). The gut microbiota shapes intestinal immune responses during health and disease. Nat. Rev. Immunol. *9*, 313–323.

Salazar-Gonzalez, R.M., Niess, J.H., Zammit, D.J., Ravindran, R., Srinivasan, A., Maxwell, J.R., Stoklasek, T., Yadav, R., Williams, I.R., Gu, X., et al. (2006). CCR6-mediated dendritic cell activation of pathogen-specific T cells in Peyer's patches. Immunity *24*, 623–632.

Sczesnak, A., Segata, N., Qin, X., Gevers, D., Petrosino, J.F., Huttenhower, C., Littman, D.R., and Ivanov, I.I. (2011). The genome of th17 cell-inducing segmented filamentous bacteria reveals extensive auxotrophy and adaptations to the intestinal environment. Cell Host Microbe *10*, 260–272.

Smith, K., McCoy, K.D., and Macpherson, A.J. (2007). Use of axenic animals in studying the adaptation of mammals to their commensal intestinal microbiota. Semin. Immunol. *19*, 59–69.

Snel, J., Heinen, P.P., Blok, H.J., Carman, R.J., Duncan, A.J., Allen, P.C., and Collins, M.D. (1995). Comparison of 16S rRNA sequences of segmented filamentous bacteria isolated from mice, rats, and chickens and proposal of "Candidatus Arthromitus". Int. J. Syst. Bacteriol. *45*, 780–782.

Turnbaugh, P.J., Ley, R.E., Hamady, M., Fraser-Liggett, C.M., Knight, R., and Gordon, J.I. (2007). The human microbiome project. Nature *449*, 804–810.

Turnbaugh, P.J., Hamady, M., Yatsunenko, T., Cantarel, B.L., Duncan, A., Ley, R.E., Sogin, M.L., Jones, W.J., Roe, B.A., Affourtit, J.P., et al. (2009a). A core gut microbiome in obese and lean twins. Nature *457*, 480–484.

Turnbaugh, P.J., Ridaura, V.K., Faith, J.J., Rey, F.E., Knight, R., and Gordon, J.I. (2009b). The effect of diet on the human gut microbiome: a metagenomic analysis in humanized gnotobiotic mice. Sci. Transl. Med. *1*, 6ra14.

Umesaki, Y., Setoyama, H., Matsumoto, S., Imaoka, A., and Itoh, K. (1999). Differential roles of segmented filamentous bacteria and clostridia in development of the intestinal immune system. Infect. Immun. *67*, 3504–3511.

Vaishnava, S., Behrendt, C.L., Ismail, A.S., Eckmann, L., and Hooper, L.V. (2008). Paneth cells directly sense gut commensals and maintain homeostasis at the intestinal host-microbial interface. Proc. Natl. Acad. Sci. USA *105*, 20858–20863.

Vaishnava, S., Yamamoto, M., Severson, K.M., Ruhn, K.A., Yu, X., Koren, O., Ley, R., Wakeland, E.K., and Hooper, L.V. (2011). The antibacterial lectin RegIIIgamma promotes the spatial segregation of microbiota and host in the intestine. Science *334*, 255–258.

Wen, L., Ley, R.E., Volchkov, P.Y., Stranges, P.B., Avanesyan, L., Stonebraker, A.C., Hu, C., Wong, F.S., Szot, G.L., Bluestone, J.A., et al. (2008). Innate immunity and intestinal microbiota in the development of type 1 diabetes. Nature *455*, 1109–1113.

Wills-Karp, M., Santeliz, J., and Karp, C.L. (2001). The germless theory of allergic disease: revisiting the hygiene hypothesis. Nat. Rev. Immunol. *1*, 69–75.

Wu, H.J., Ivanov, I.I., Darce, J., Hattori, K., Shima, T., Umesaki, Y., Littman, D.R., Benoist, C., and Mathis, D. (2010). Gut-residing segmented filamentous bacteria drive autoimmune arthritis via T helper 17 cells. Immunity *32*, 815–827.

Yang, X.O., Pappu, B.P., Nurieva, R., Akimzhanov, A., Kang, H.S., Chung, Y., Ma, L., Shah, B., Panopoulos, A.D., Schluns, K.S., et al. (2008). T helper 17 lineage differentiation is programmed by orphan nuclear receptors ROR alpha and ROR gamma. Immunity *28*, 29–39.

EXTENDED EXPERIMENTAL PROCEDURES

DNA Extraction, 16S rDNA Amplification, and Multiplex Pyrosequencing

Fecal materials were stored at –80°C before processing, and bulk DNA was extracted from mouse fecal pellets and inoculum pools with the QIAamp DNA Stool Mini Kit (QIAGEN, Valencia, CA) according to the manufacturer's recommendations. In brief, frozen fecal pellets were weighed and then thoroughly resuspended in Buffer ASL (QIAGEN). For the extraction of DNA from inoculum pools, aliquots (200 μl) of ice-cold suspension were thoroughly resuspended in Buffer ASL. Following extraction, DNA was eluted in 150 μl of elution buffer and stored at –20°C. Controls—i.e., tubes containing only the QIAamp DNA Stool Mini Kit components—were included throughout the DNA extraction and PCR steps to monitor for possible contamination. Amplification of the V1-V2-V3 region of the 16S rDNA was performed essentially as described previously (Dethlefsen and Relman, 2011). In brief, PCR was undertaken with 50 ng of template DNA in 50-μl reactions with fusion primers comprised of A linker–10-mer barcode–dinucleotide spacer–533–515R reverse primer and B linker–dinucleotide spacer–8–27F forward primer, as described (Roche). PCR products were gel purified as described (QIAGEN) and were quantified with Quant-iT PicoGreen (Invitrogen); samples were pooled in equal ratios. Amplicon length distributions and concentrations were determined with a Bioanalyzer (Agilent, Palo Alto, CA), and the pool was submitted for GS-FLX Titanium pyrosequencing (Roche).

Analysis of 16S rDNA Sequences

Over 1.1 million raw pyrosequencing reads were obtained, filtered, and quality-trimmed as previously described (Dethlefsen and Relman, 2011) with mothur (Schloss et al., 2009). In brief, reads with more than one ambiguous character were removed, the proximal primer and barcode sequences were trimmed off, and reads shorter than 390 bp and longer than 520 bp were discarded. These steps resulted in a total of 808,810 reads that could be assigned unambiguously to a sample. The numbers of sequences are summarized in Table S4.

Phylogenetic assignments were obtained by clustering reads with Uclust (http://www.drive5.com/) (Edgar, 2010) at a maximum distance of 5% with the Needleman–Wunsch algorithm based on a high-quality seed library. The seed library consisted of 47,768 high-quality sequences derived from a pre-clustered SILVA SSU rRNA reference database release 100 (http://www.arb-silva.de/). Omitted from further analysis were 127,176 reads that did not cluster with a seed within a genetic distance of 5%. A total of 681,634 reads clustered with a reference sequence, of which 462 reads were singletons and therefore were discarded. The remaining 681,172 reads were assigned to a total of 1,866 OTUs. There were 546,855 reads with $\geq$ 99% similarity to their respective seed (refOTU); these reads were assigned to 1,113 OTUs. The 112,333 reads that were 98.9%–98% similar to a seed were assigned to 371 OTUs, the 14,862 reads that were 97.9%–97% similar to a seed were assigned to 189 OTUs, the 6,579 reads that were 96.9%–96% similar to a seed were assigned to 129 OTUs, and the 543 reads that were 95.9%–95% similar to a seed were assigned to 64 OTUs. In this study, the term *operational taxonomic unit* (OTU) is used synonymously with the term *bacterial species*. As described, OTUs were defined on the basis of sequence clustering of V1-V2-V3 16S rDNA pyrosequence reads with a high-quality reference database. To evaluate differences between microbial communities, unweighted UniFrac distances—i.e., a phylogenetic beta diversity metric (Lozupone and Knight, 2005)—were calculated from normalized read numbers per sample between all pairs of samples. The relatedness of community membership in each sample was assessed through principal coordinates analysis with the QIIME software package (Quantitative Insights Into Microbial Ecology, http://qiime.sourceforge.net/) (Caporaso et al., 2010). The sequence data used for these analyses are available at http://sites.google.com/site/davidrelmanlab/databases/supplements.

Quantitative rDNA Analysis

For qPCR on genomic DNA extracted from fecal specimens (see above), fluorescent primer- and probe-based chemistry and a StepOnePlus Real-Time PCR System (Applied Biosystems) were used. For broad-range bacterial qPCR, primers Bact8FM/8FB and Bact515R and probe Bact338K were used (Palmer et al., 2007). For SFB-specific qPCR, the primers and the probe were designed to detect SFB originating from a variety of hosts. Primers SFB735F (5-CTTACTGGACTGTAACTGAC-3) and SFB1266R (5-TAAGTTTTGCTCACTATCRC-3) and probe SFB995 (FAM-5-CATACCTTGAATTACCTTGTAATGAGGGA-3-TAMRA) were designed on the basis of the high-quality SFB 16S rDNA sequences of the SILVA SSU reference database release 100 (http://www.arb-silva.de/). Primers and probe specificities were checked with RDP ProbeMatch (http://rdp.cme.msu.edu/probematch/search.jsp) and probeCheck (http://131.130.66.200/cgi-bin/probecheck/content.pl?id=home). In the establishment phase of this assay, PCR products were cloned and sequenced to evaluate possible false-positive amplifications. No other clostridial or bacterial 16S rDNA sequences other than SFB-specific 16S rDNA sequences were detected. To obtain an SFB-positive control, 16S rDNA was amplified from fecal material from an SFB-monocolonized mouse with primers Bact8FMxBact1391R (Palmer et al., 2007), cloned into pCR2.1-TOPO (Invitrogen), and sequenced. To create a positive control for broad-range bacterial 16S rDNA PCR, 16S rDNA was amplified from *Escherichia coli* with primers Bact8FMxBact1391R, cloned into pCR2.1-TOPO (Invitrogen), and sequenced. This plasmid was used in triplicate at 10-fold dilutions in each qPCR run to generate standard curves. Each DNA extract was analyzed in three independent qPCR assays. The following thermal cycling protocol was used for amplifications: 50°C for 2 min and 95°C for 10 min, followed by 40 cycles of 95°C for 30 s, 55°C for 30 s, 60°C for 45 s, 65°C for 15 s, and 72°C for 15 s. rDNA copy numbers were determined from the standard curves with SDS software (Applied Biosystems), with the baseline and cycle threshold set according to

the manufacturer's recommendations, and were calculated as 16S rDNA copy numbers per gram of fecal sample or as 16S rDNA copy numbers per milliliter of inoculum.

Cohousing Experiments

HMb mice (6-8 weeks old) were co-housed for 4 weeks with MMb or SFB-monocolonized mice in a sterile cage with autoclaved food and water. As a negative control, a cage housing HMb mice only was maintained under the same sterile conditions. HMb mice from different cohousing conditions were sacrificed after 4 weeks for analysis of T cell numbers in the IEL, LP, and PP compartments.

Colonization of GF Mice with Ten Human Samples

Human fecal samples were collected from 10 donors (H10 inoculum), pooled, weighed, and resuspended in PBS to 10% (by g/ml). All human donors were free of antibiotic treatment. H10 inoculum (200 μl) was administered by oral gavage to 3-4 week old GF mice. As a positive and negative control, GF mice were gavaged with mouse inoculum (M inoculum) or human inoculum (H inoculum, from the initial two human donors), respectively. Mice were sacrificed after 4 weeks of colonization for gut T cell number analysis.

Immunohistochemistry

Segments of jejunum from 9- to 12-week-old MMb, HMb, and GF mice were flushed and embedded in OCT mounting medium (Tissue Tek) and were snap-frozen in isopropanol and dry ice. Sections (5 μm thick) were attached to glass slides, air-dried overnight (ON), and fixed twice with ice-cold acetone for 10 min. Sections were blocked with 5% goat serum/0.1% Tween at room temperature for 1 hr and stained with 1:100 anti-CD3ε antibody (BD Biosciences, San Jose, CA) at 37°C for 2 hr. The sections were washed with PBS and incubated with 1:100 FITC-conjugated anti-Armenian Hamster IgG (Jackson Laboratories, Bar Harbor, ME) for 1.5 hr at 37°C. Lastly, slides were washed with PBS and counterstained with DAPI. IgA staining of intestinal sections has been previously described (Mombaerts et al., 1993). In brief, incubation of intestinal sections with biotin anti-mouse IgA (BD Biosciences) at a 1:50 dilution for 1 hr was followed by sequential incubations with the avidin-biotinylated peroxidase reagent (Vector, Burlingame, CA). Each incubation was followed by three washes in PBS (pH 7.4). The tissue sections were stained by incubation in a solution of 3-amino-9-ethylcarbazole (Aldrich, Milwaukee, WI) to develop red deposits, counterstained with hematoxylin, and mounted in glycergel (DAKO).

DC/T Cell Coculture Assays

MMb and HMb mice were injected with 20 million Flt3L-secreting tumor cells to expand DC populations. After 3 weeks, mice were sacrificed. MLNs, PPs, and peripheral lymph nodes (PLNs, a pool of inguinal and brachial lymph nodes) were digested with HBSS/Liberase (Roche, 0.5 mg/ml)/DNase (Sigma, 0.2 mg/ml) for 1 hr at 37°C, and DCs were isolated by positive selection with CD11c microbeads (Miltenyi, Auburn, CA). Isolated DCs were pre-incubated with a P14 peptide (New England Biolabs, Ipswich, MA), gp_{33-41} peptide from lymphocytic choriomeningitis virus (LCMV), at a 1:100 dilution (5 μl of peptide/500 μl of IMDM) at 37°C for 2 hr. After incubation, the peptide solution was washed and the cell concentration adjusted to 10^6/ml in IMDM. A 100-μl volume of DCs was added to a 96-well flat plate. P14-specific transgenic $CD8^+$ T cells from mice with a TCRα−/− background (TCR-LCMV-P14/TCRα−/−, Taconic) were isolated from the spleen and incubated with DCs at a 1:1 ratio. Positive control wells contained DCs (no P14 peptide incubation), P14 $CD8^+$ T cells, and retinoic acid (RA, 100 nM). After co-culture for 4–5 days, expression of CCR9 and α4β7 in P14 $CD8^+$ T cells was measured by flow cytometry.

Adoptive Transfer Experiments

Plates with six wells were coated overnight at 4°C with azide-free anti-CD3 and anti-CD28 (1 μg/ml; BD Biosciences) antibodies. $CD4^+$ T cells from SPF SW mice were purified by negative selection with CD4 microbeads (Miltenyi). $CD4^+$ T cells (2×10^6/ml) were incubated with or without RA (100 nM) in RPMI complete medium. On day 3, the anti-CD3, CD28 stimulation was removed, and cells were washed, split, and incubated with IL-2 (50 U/ml). On day 5, RA-untreated cells were stained with CFSE and RA-treated cells with CMTMR. Cells were resuspended in PBS (10^6/100 μl) for injection. Equal numbers of cells from the two populations were mixed (input) and adoptively transferred into MMb or HMb mice (200 μl per mouse). Mice were killed 10 hr after injection, and single-cell suspensions of the MLNs, PPs, LP, spleen, and PLNs were analyzed by flow cytometry to measure the ratio of $CFSE^+$ to $CMTMR^+$ in each anatomic location.

Microarray Analysis

CD4+ T cells were isolated from spleen, MLNs, and small-intestinal LP of 10- to 14-week-old individual mice, as described previously (Feuerer et al., 2010). Cells were sorted (BD FACSAria) into TRIzol on the basis of the following cell surface markers: CD45+, CD8a-, CD11b-CD11c-CD19-B220-GR-1-, TCRβ+, and CD4+. In addition, a segment of the ileum (1–2 cm) was excised and stored in TRIzol at –80°C. RNA was extracted and then amplified, labeled, and hybridized to Affymetrix GeneChip Mouse Gene 1.0 ST arrays (Expression Analysis, Durham, NC). Raw data were normalized with the RMA algorithm implemented in the Expression File Creator module from the GenePattern suite (Reich et al., 2006). Data were visualized with the Multiplot and Hierarchical Clustering Viewer modules. All cell populations analyzed were generated at least in triplicate from independent experiments.

Real-Time qPCR Analysis

The small intestine from 9- to 12-week-old mice was dissected, and PPs were excised. The remaining small-intestinal tissue was incubated with 1 mM DTT/1 mM EDTA/3% FBS/PBS for 30 min at 37°C for extraction of the epithelial layer. Epithelial cells were incubated first at 4°C for 1 day in RNAlater solution (Ambion, Austin, TX) and then at –80°C until RNA extraction. RNA was extracted with an RNeasy Mini Kit (QIAGEN) and treated with TURBO DNA-*free* DNase Treatment and Removal Reagents (Ambion). RNA was retrotranscribed with an iScript cDNA synthesis kit (Bio-Rad, Hercules, CA), and qPCR was performed with SYBR Green RT-PCR (Fermentas, Glen Burnie, MD). The following primers were used: GAPDH-F: 5′CCTCGTCCCGTAGACAAAATG; GAPDH-R: 5′TCTCCACTTTGCCACTGCAA; 18S rDNA-F: 5′CATTCGAACGTCTGCCCTATC; 18S rDNA-R: 5′CCTGCTGCCTTCCTTGGA; RegIIIγ-F: 5′TTCCTGTCCTCCATGATCAAAA; RegIIIγ-R: 5′CATCCACCTCTGTTGGGTTCA; CCL28-F: 5′CAGCCCGCACAATCG TACT; CCL28-R: 5′ACGTTTTCTCTGCCATTCTTCTTT; CXCL9-F: 5′AATGCACGATGCTCCTGCA; CXCL9-R: 5′AGGTCTTTGAGG GATTTGTAGTGG; CCL20-F: 5′TTTTGGGATGGAATTGGACAC; CCL20-R: 5′TGCAGGTGAAGCCTTCAACC. The comparative Ct method was used to quantify transcripts that were normalized with respect to GAPDH or 18S rDNA.

TUNEL Assay

Staining of single-cell suspensions of PPs and MLNs with antibody to CD3 was followed by TUNEL staining with the In Situ Cell Death Detection Kit, Fluorescein (Roche). Results were analyzed by flow cytometry.

SUPPLEMENTAL REFERENCES

Caporaso, J.G., Kuczynski, J., Stombaugh, J., Bittinger, K., Bushman, F.D., Costello, E.K., Fierer, N., Peña, A.G., Goodrich, J.K., Gordon, J.I., et al. (2010). QIIME allows analysis of high-throughput community sequencing data. Nat. Methods *7*, 335–336.

Dethlefsen, L., and Relman, D.A. (2011). Incomplete recovery and individualized responses of the human distal gut microbiota to repeated antibiotic perturbation. Proc. Natl. Acad. Sci. USA *108* (*Suppl 1*), 4554–4561.

Edgar, R.C. (2010). Search and clustering orders of magnitude faster than BLAST. Bioinformatics *26*, 2460–2461.

Feuerer, M., Hill, J.A., Kretschmer, K., von Boehmer, H., Mathis, D., and Benoist, C. (2010). Genomic definition of multiple ex vivo regulatory T cell subphenotypes. Proc. Natl. Acad. Sci. USA *107*, 5919–5924.

Iwata, M., Hirakiyama, A., Eshima, Y., Kagechika, H., Kato, C., and Song, S.Y. (2004). Retinoic acid imprints gut-homing specificity on T cells. Immunity *21*, 527–538.

Lozupone, C., and Knight, R. (2005). UniFrac: a new phylogenetic method for comparing microbial communities. Appl. Environ. Microbiol. *71*, 8228–8235.

Mombaerts, P., Mizoguchi, E., Grusby, M.J., Glimcher, L.H., Bhan, A.K., and Tonegawa, S. (1993). Spontaneous development of inflammatory bowel disease in T cell receptor mutant mice. Cell *75*, 274–282.

Mora, J.R., Bono, M.R., Manjunath, N., Weninger, W., Cavanagh, L.L., Rosemblatt, M., and Von Andrian, U.H. (2003). Selective imprinting of gut-homing T cells by Peyer's patch dendritic cells. Nature *424*, 88–93.

Palmer, C., Bik, E.M., DiGiulio, D.B., Relman, D.A., and Brown, P.O. (2007). Development of the human infant intestinal microbiota. PLoS Biol. *5*, e177.

Reich, M., Liefeld, T., Gould, J., Lerner, J., Tamayo, P., and Mesirov, J.P. (2006). GenePattern 2.0. Nat. Genet. *38*, 500–501.

Schloss, P.D., Westcott, S.L., Ryabin, T., Hall, J.R., Hartmann, M., Hollister, E.B., Lesniewski, R.A., Oakley, B.B., Parks, D.H., Robinson, C.J., et al. (2009). Introducing mothur: open-source, platform-independent, community-supported software for describing and comparing microbial communities. Appl. Environ. Microbiol. *75*, 7537–7541.

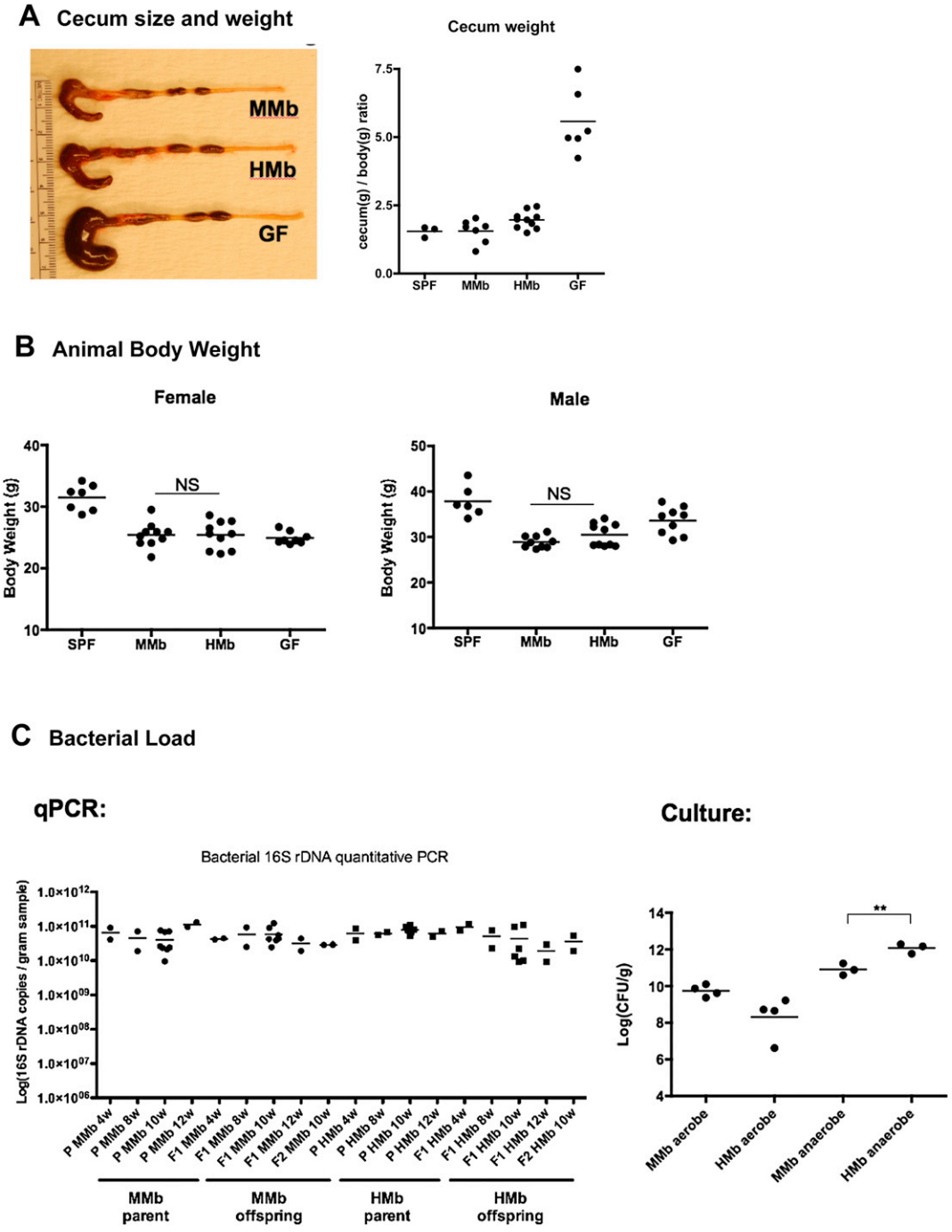

Figure S1. Physical Properties and Microbiota of MMb versus HMb Mice, Related to Figure 1

(A) Cecum size (*left*) and ratio of cecum weight to body weight (*right*) for MMb, HMb, SPF, and GF mice.

(B) Body weight in age-comparable MMb, HMb, SPF, and GF mice, by sex.

(C) *Left:* Abundance of bacteria in parent (P), first offspring (F1), and second offspring (F2) generations of MMb and HMb mice, measured as bacterial 16S rDNA copy numbers by qPCR. *Right:* Bacterial colony-forming units (CFU) per gram of feces obtained through cultivation under aerobic and anerobic conditions. In (A)–(C), each dot or square represents an individual mouse. Horizontal bars indicate the means, and *P* values were calculated by unpaired/two-tailed t test. **p < 0.01, NS = not significant by t test.

(D) Heat map displaying the relative abundance of all 1,866 OTUs detected in MMb and HMb mice from the parent (P0), first offspring (F1), and second offspring (F2) generations. Each column represents an individual mouse. Colors represent phylum membership of OTUs, and bacterial clades are indicated to the right. Other phyla (gray) are Lentisphaerae, 4C0d-2, TM7, and Deferribacteres.

(E) Number of shared OTUs within each major bacterial phylum in MMb and HMb inoculum samples.

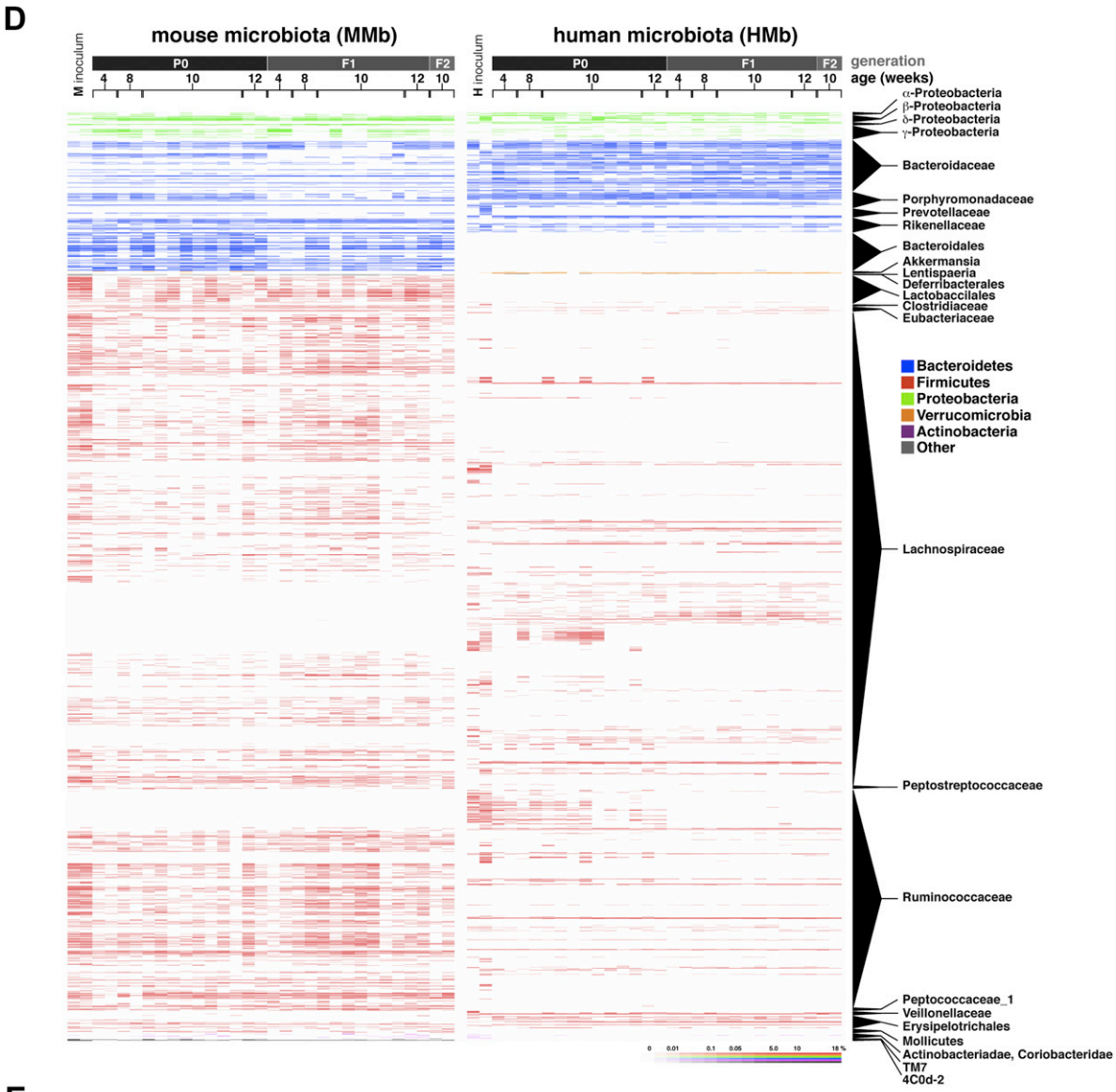

Figure S1. (*continued*).

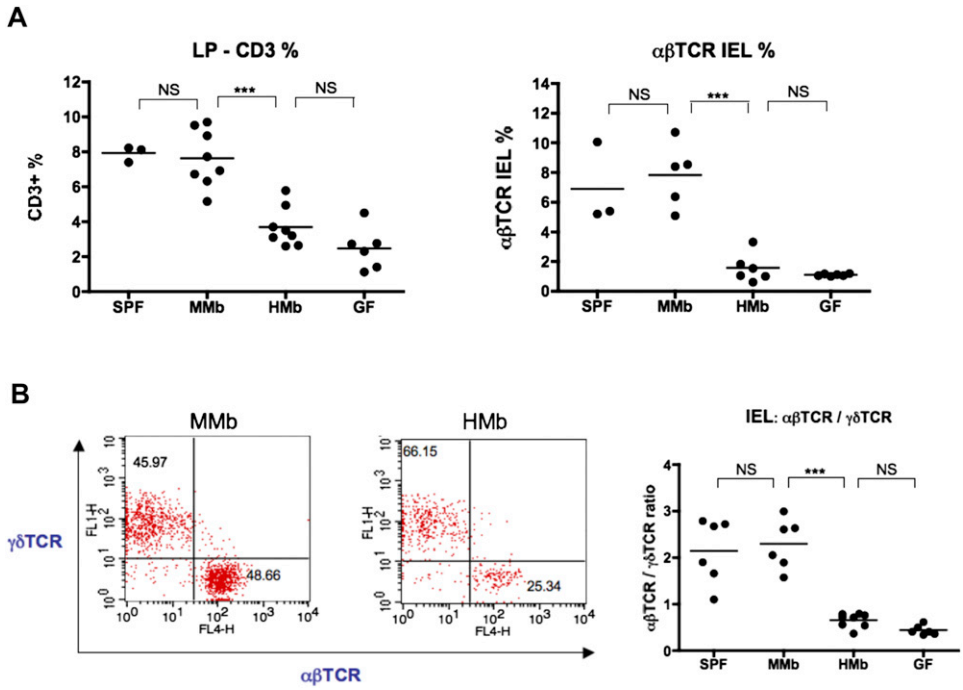

Figure S2. Percentage and Ratio of T Cells in the Small Intestinal Tissue, Related to Figure 2

(A) Percentage of total small-intestinal LP cells accounted for by $CD3^+$ cells (*left panel*) and the percentage of total purified cells from the small-intestinal epithelial layer accounted for by $TCR\beta^+CD103^+$ cells (*right panel*) were measured by flow cytometry.

(B) Ratio of αβTCR IELs to γδTCR IELs. IELs were extracted from the small intestine and stained with antibodies to CD3 and CD103. $CD3^+CD103^+$ cells were further stained with antibodies to TCRβ and TCRγδ to identify αβTCR IELs and γδTCR IELs, respectively. The two left panels show representative results for MMb and HMb mice. Numbers indicate percentages of cells in the quadrant of total $CD3^+CD103^+$ cells. The right panel shows a collective result for the αβTCR/γδTCR ratio. Each dot represents an individual mouse. Horizontal bars indicate the means. *P* values were calculated by unpaired/two-tailed t test. ***$p < 0.001$, NS = not significant by t test.

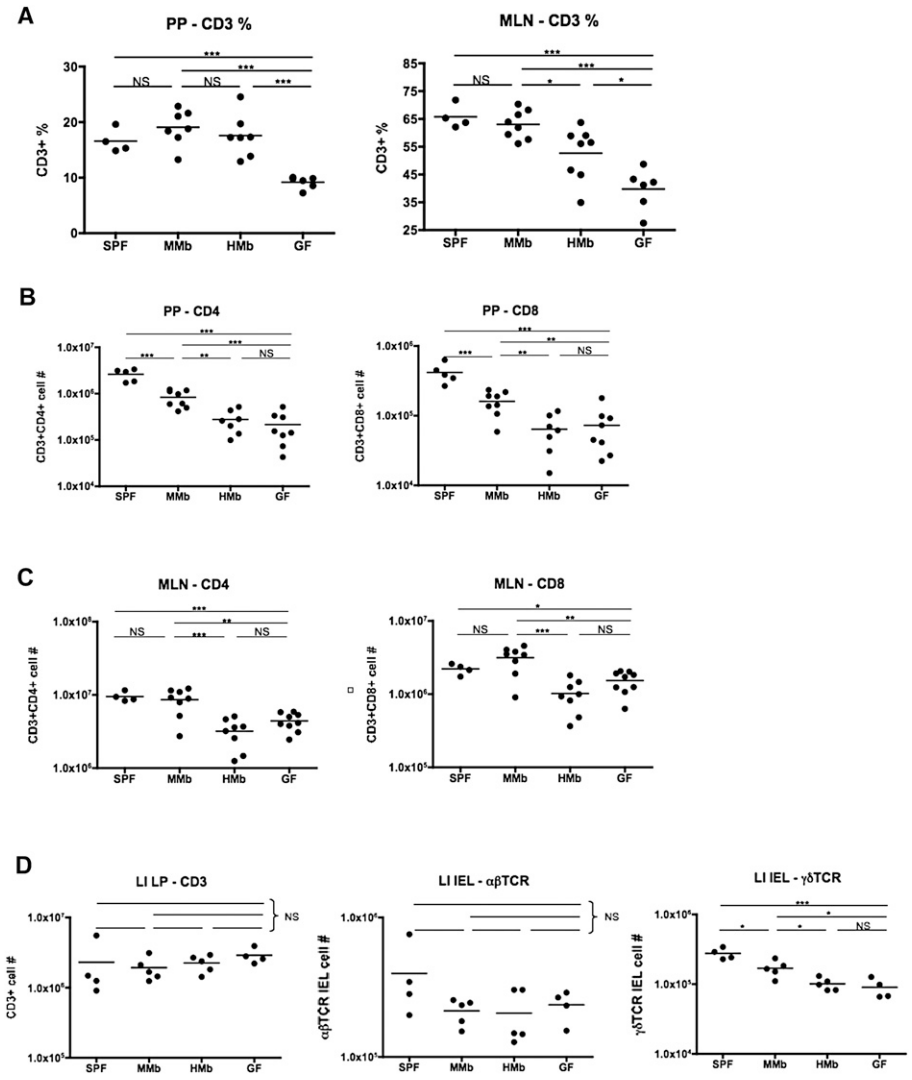

Figure S3. MMb, but Not HMb, Increases T Cell and Dendritic Cell Populations and Antimicrobial Peptide Expression in the Small Intestine, Related to Figure 3

(A) The $CD3^+$ cell percentages among total PP cells (*left panel*) and total MLN cells (*right panel*) were measured by flow cytometry.

(B and C) Single-cell suspensions of PPs and MLNs were prepared and stained with fluorescently labeled antibodies to CD3, CD4, and CD8, with subsequent flow cytometry to measure absolute numbers of $CD3^+CD4^+$ and $CD3^+CD8^+$ cells in the PPs (B) and MLNs (C).

(D) Absolute T cell numbers in the large-intestinal (LI) tissue were measured by flow cytometry. IELs were extracted from the large intestine and stained with antibodies to CD3, CD103, TCRβ, and TCRγδ to measure numbers of αβTCR IELs and γδTCR IELs (*middle and right panels*). The remaining LI LP tissue was digested, and single-cell suspensions of LI LP cells were stained for CD3 (*left panel*).

(E) Single-cell suspensions of inguinal and brachial lymph nodes were prepared and stained with antibody to CD3, with subsequent flow cytometry to measure absolute numbers of T cells.

(F) Dendritic cell (DC) populations in the LP, PPs, and MLNs of MMb, HMb, and GF mice. Single-cell suspensions of LP tissue were prepared by digestion of small-intestinal tissue with collagenase/dispase after IEL extraction. PPs and MLNs were also digested with collagenase/dispase to ensure optimal extraction of DCs from the stromal layer. Single-cell suspensions were stained with fluorescently labeled antibodies to CD11c, CD11b, and F4/80 and then subjected to flow cytometry. The dot plot demonstrates a representative gating strategy for DCs (*left panel*). $CD11c^{high}$ cells (R3 gate) were designated as DCs. To exclude other $CD11c^+$ monocytes, $CD11c^{low/int}$ $CD11b^{high}$ (R2 gate) cells were excluded from the analysis. Of note, when F4/80 expression was analyzed, $CD11c^{low/int}$ $CD11b^{high}$ cells had a mean fluorescence intensity (MFI) three fold higher than the F4/80 MFI of $CD11c^{high}$ cells, suggesting $CD11c^{low/int}$ $CD11b^{high}$ are mostly macrophages, not DCs. MMb, HMb, and GF mice were all processed in parallel, and absolute $CD11c^{high}$ cell numbers in MMb and HMb mice were normalized to those in GF mice (3–5 mice per group).

(G) Expression of the antimicrobial peptide RegIIIγ was examined by microarray analysis of the ileal tissue (*left panel*). Results from microarray analysis were confirmed by real-time qPCR on epithelial cells extracted from the small intestine (*right panel*). qPCR assays were run in triplicate, and results are shown as mean values normalized to 18S ribosomal RNA, and expression levels were calculated relative to GF controls. Bar graph represents two independent experiments. In panels A–G, each dot represents an individual mouse. Error bars indicate +/− SEM, and horizontal bars are means. *P* values were calculated by unpaired/two-tailed t test. $^*p < 0.05$, $^{**}p < 0.01$, $^{***}p < 0.001$, NS = not significant by t test.

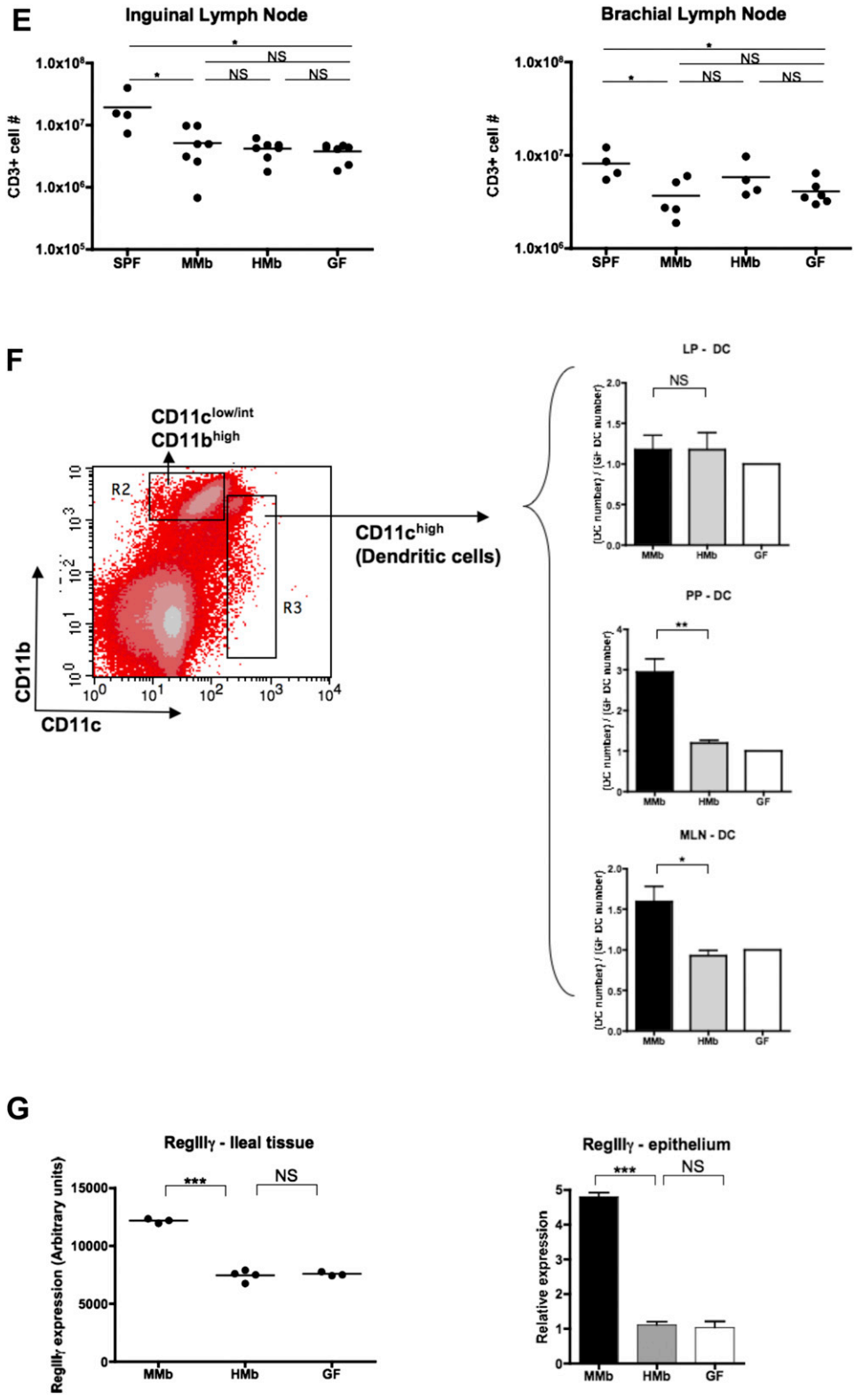

Figure S3. (*continued*).

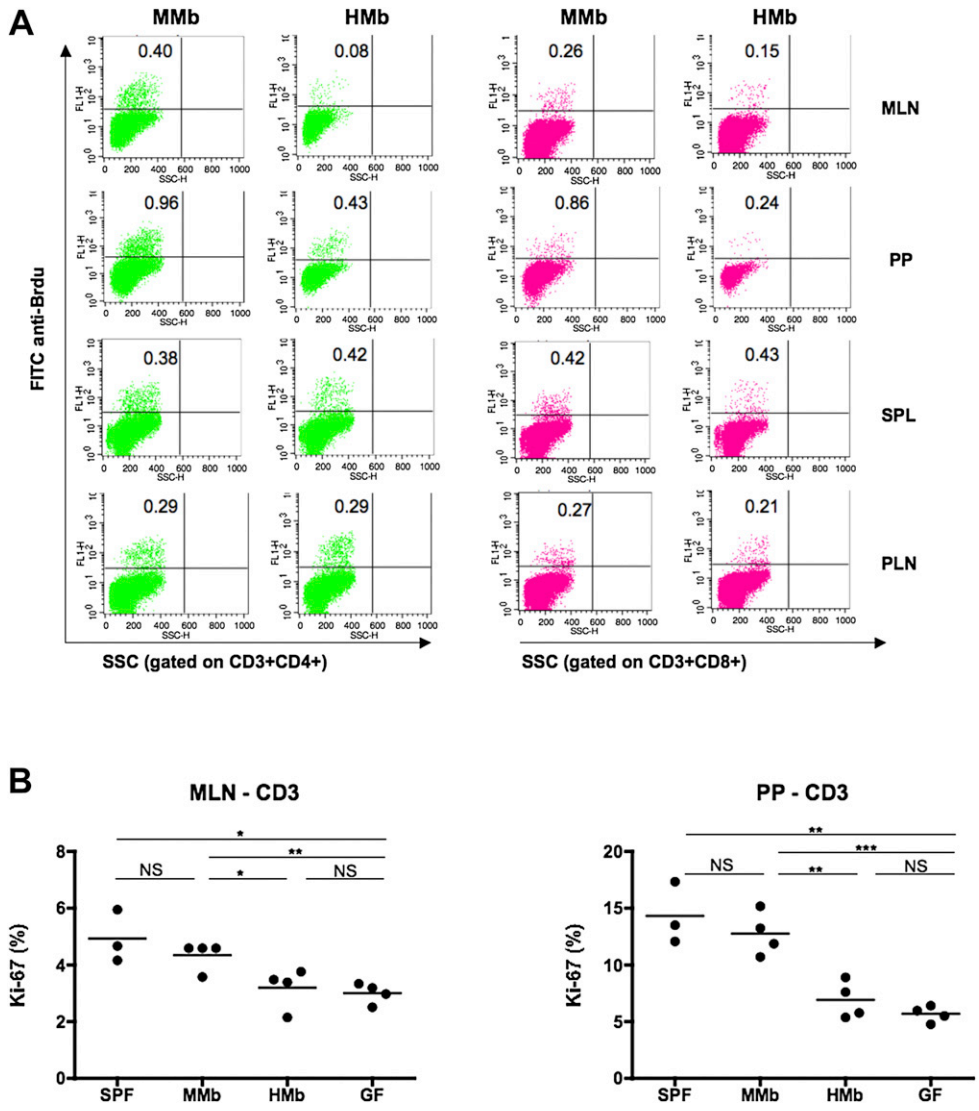

Figure S4. T Cell Proliferation, T Cell Apoptosis, and T Cell Trafficking in MMb and HMb Mice, Related to Figure 4

(A) MMb and HMb mice were injected with Brdu, which is incorporated into proliferating cells; the animals were killed 2 hr after injection. (A) $CD3^+CD4^+$ T cells (*green*) and $CD3^+CD8^+$ T cells (*pink*) in MLNs, PPs, spleen (SPL), and peripheral lymph nodes (PLNs; pooled inguinal and brachial lymph nodes) were stained with FITC-conjugated antibody to Brdu. Numbers in upper left quadrants indicate the percentages of cells positive for Brdu. SSC = side scatter.

(B) T cell proliferation was assessed by Ki-67 staining. Single-cell suspensions of PPs and MLNs were stained for CD3 and then subjected to intracellular staining with Ki-67. Results were analyzed by flow cytometry.

(C) $CD3^+Brdu^+$ cells from MLNs, PPs, and SPL in (A), were stained for the gut-homing receptors CCR9 and $\alpha4\beta7$.

(D) T cell apoptosis was assessed by TUNEL assay. Single-cell suspensions of PPs and MLNs were stained for CD3, and a TUNEL assay was performed. The TUNEL-positive cells were labeled with FITC and analyzed by flow cytometry (*upper panel*). Results of TUNEL analysis are summarized in the bar graph (*lower panel*). The percentage of TUNEL-positive cells among total $CD3^+$ cells is expressed on the *y* axis. Each group contained 3–5 mice.

(E) DCs from different anatomic sites—MLNs, PPs, and PLNs (pooled inguinal and brachial lymph nodes)—in MMb and HMb mice were cultured separately with the P14 peptide from lymphocytic choriomeningitis virus in the presence of P14-specific transgenic $CD8^+$ T cells isolated from a mouse with a TCR$\alpha-/-$ background (TCR-LCMV-P14/TCR$\alpha-/-$). After 5 days of co-culture, expression of CCR9 and $\alpha4\beta7$ was measured in P14 $CD8^+$ T cells to assess the ability of DCs to imprint gut-homing receptors on T cells. Refer to Extended Experimental Procedures for detailed protocol.

(F) Gut-homing T cells were generated in vitro by culture of naive $CD4^+$ T cells with retinoic acid (RA), which upregulates CCR9 and $\alpha4\beta7$ on T cells (Iwata et al., 2004). RA-treated and untreated cells were stained with CFSE (a green fluorophor) and CMTMR (a red fluorophor), respectively. Equal numbers of cells from the two populations were mixed (input) and adoptively transferred into MMb or HMb mice. Mice were killed 10 hr after injection, and single-cell suspensions of the MLNs, PPs, LP, SPL, and PLNs were analyzed by flow cytometry to measure the ratio of $CFSE^+$ to $CMTMR^+$ cells in each anatomic location. Intestinal homing efficiency of the transferred cells to different anatomic locations was measured by calculating the "homing index"—the ratio of $CFSE^+$ to $CMTMR^+$ cells corrected for input ratio—as previously demonstrated (Mora et al., 2003). Each group contained 3–5 mice. Refer to Extended Experimental Procedures for detailed protocol.

(G) Expression of MAdCAM and CCL25 was examined by microarray analysis of the ileal tissue. In panels C, D, and F, *P* values were calculated by unpaired/two-tailed t test. *$p < 0.05$, **$p < 0.01$, ***$p < 0.001$, NS = not significant by t test.

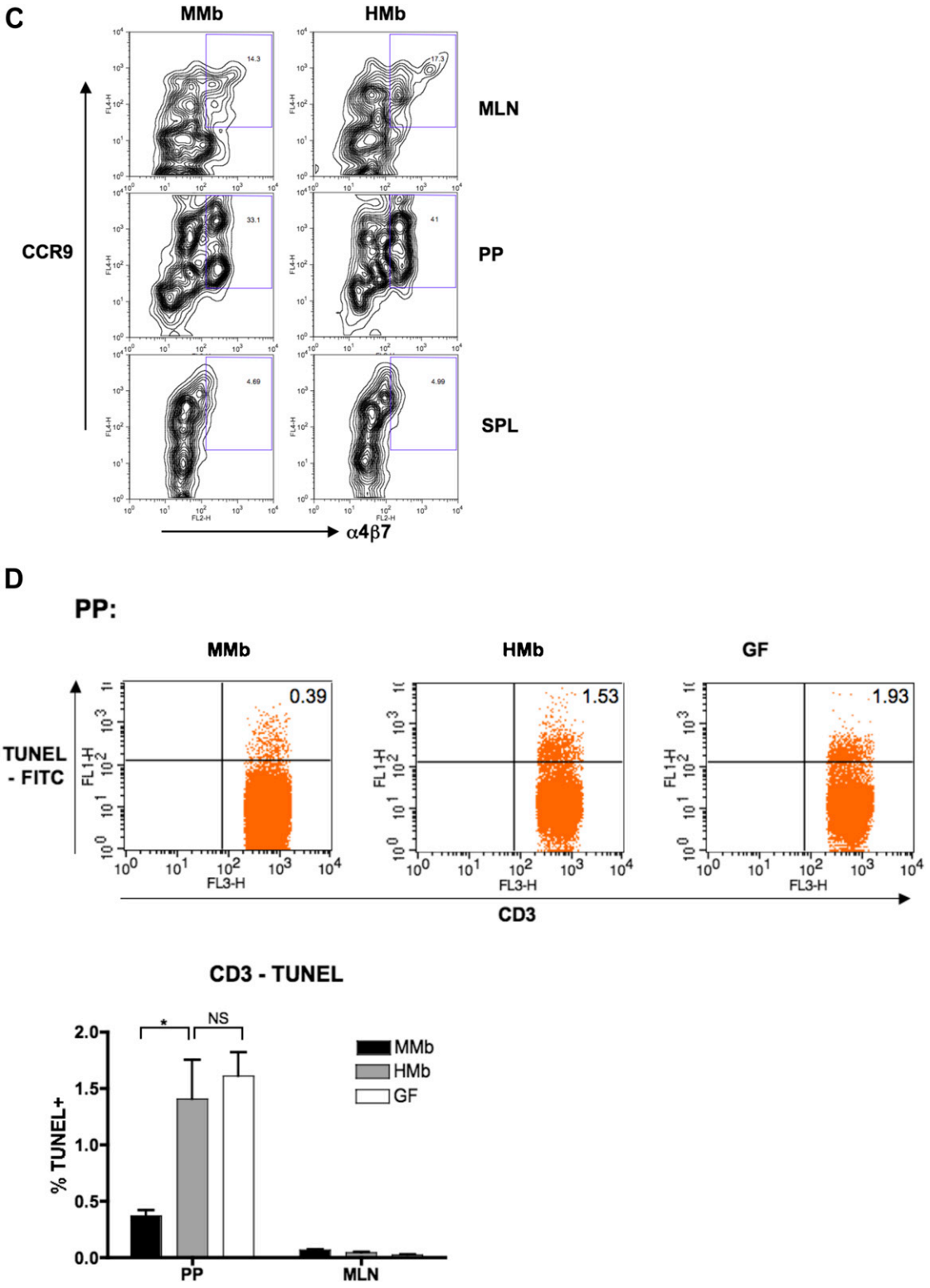

Figure S4. (*continued*).

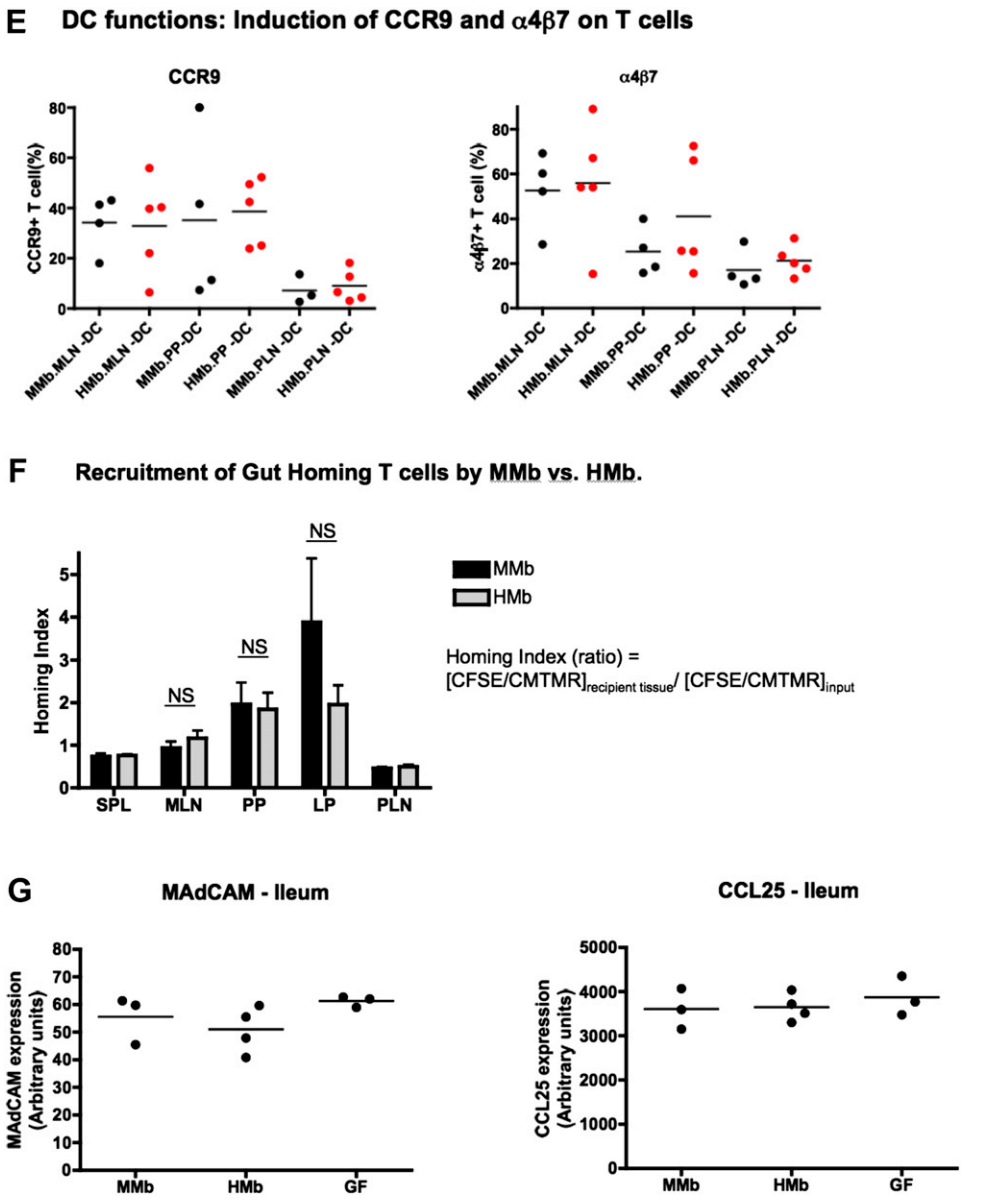

Figure S4. (*continued*).

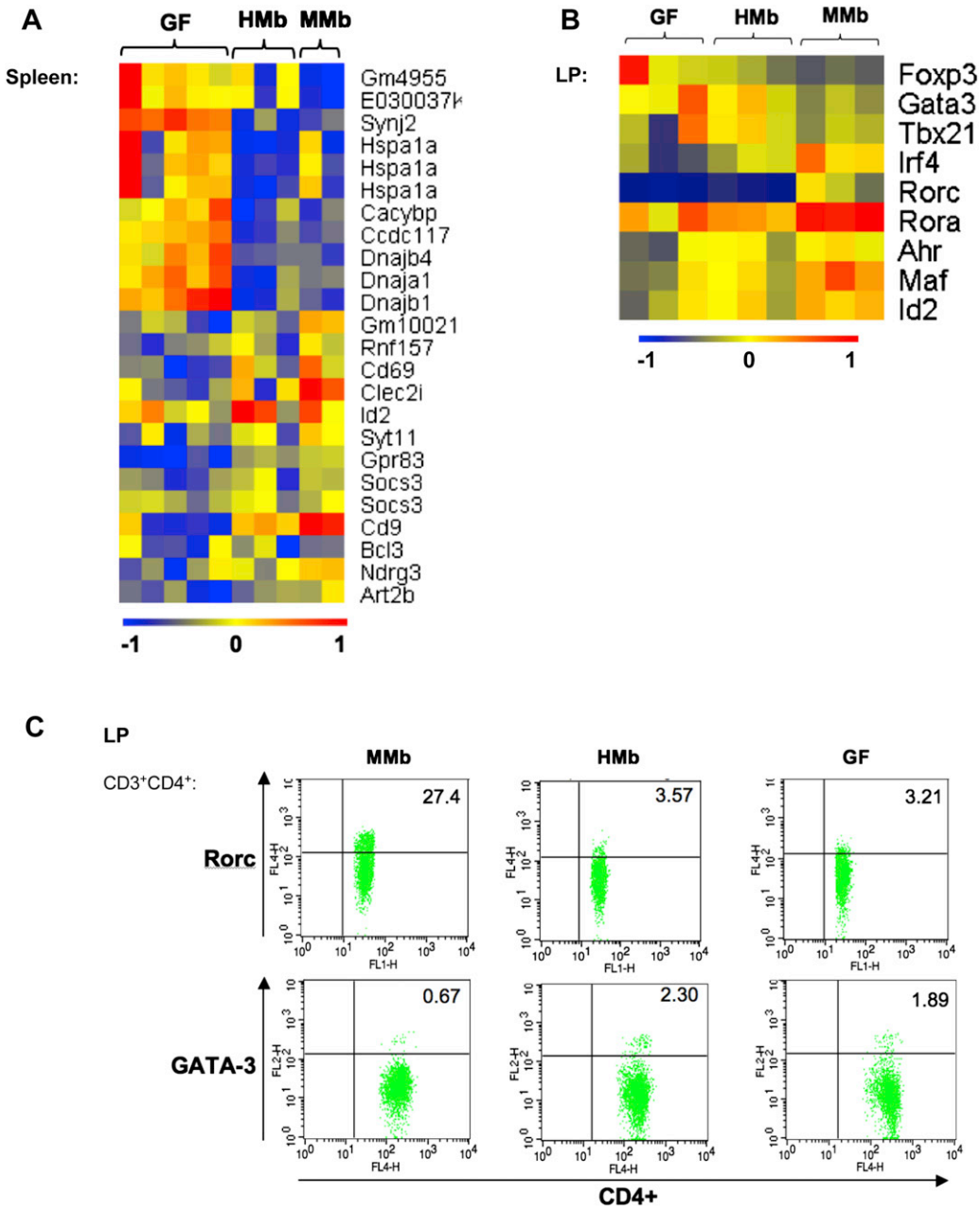

Figure S5. Microarray Analysis of CD4$^+$ T Cells from LP and Intestinal Tissue of MMb, HMb, and GF Mice, Related to Figure 5

(A and B) The heat map shows differentially expressed transcription factors in CD4$^+$ T cells sorted from the spleen (A) or small-intestinal LP (B). Genes with the highest and lowest levels of transcripts are colored in red and blue, respectively.

(C) Single-cell suspensions of LP tissue (after IEL extraction) were stained with antibodies to CD3 and CD4, with subsequent intracellular staining for transcription factors Rorc and GATA-3.

(D) Relative expression of B cell specific–genes was examined by microarray analysis in the ileum. A total of 49 B cell–specific genes were selected from the ImmGen data set on the basis of their highest differential expression in B cells. Each dot represents an individual gene, and each column is an individual mouse.

(E) Small-intestinal sections were immunohistochemically labeled for IgA$^+$ cells. Intestinal sections were stained with biotin anti-mouse IgA. The sections were sequentially incubated with the avidin-peroxidase reagent, developed with the substrate of 3-amino-9-ethylcarbazole, and counterstained with hematoxylin. The red deposits indicate IgA$^+$ cells.

(F) Relative expression of the chemokines CCL20, CXCL9, and CCL28 was examined in ileal tissue by microarray analysis (*upper panels*). Microarray data were confirmed by qPCR of epithelial cells purified from the small intestine of MMb, HMb, and GF mice (*lower panels*). qPCR assays were run in triplicate, and results are shown as mean values normalized to GAPDH, and expression levels were calculated relative to GF controls. Bar graphs represent two independent experiments. In panel F, each dot represents an individual mouse. Horizontal bars indicate the means. *P* values were calculated by unpaired/two-tailed t test. *$p < 0.05$, **$p < 0.01$, ***$p < 0.001$, NS = not significant by t test.

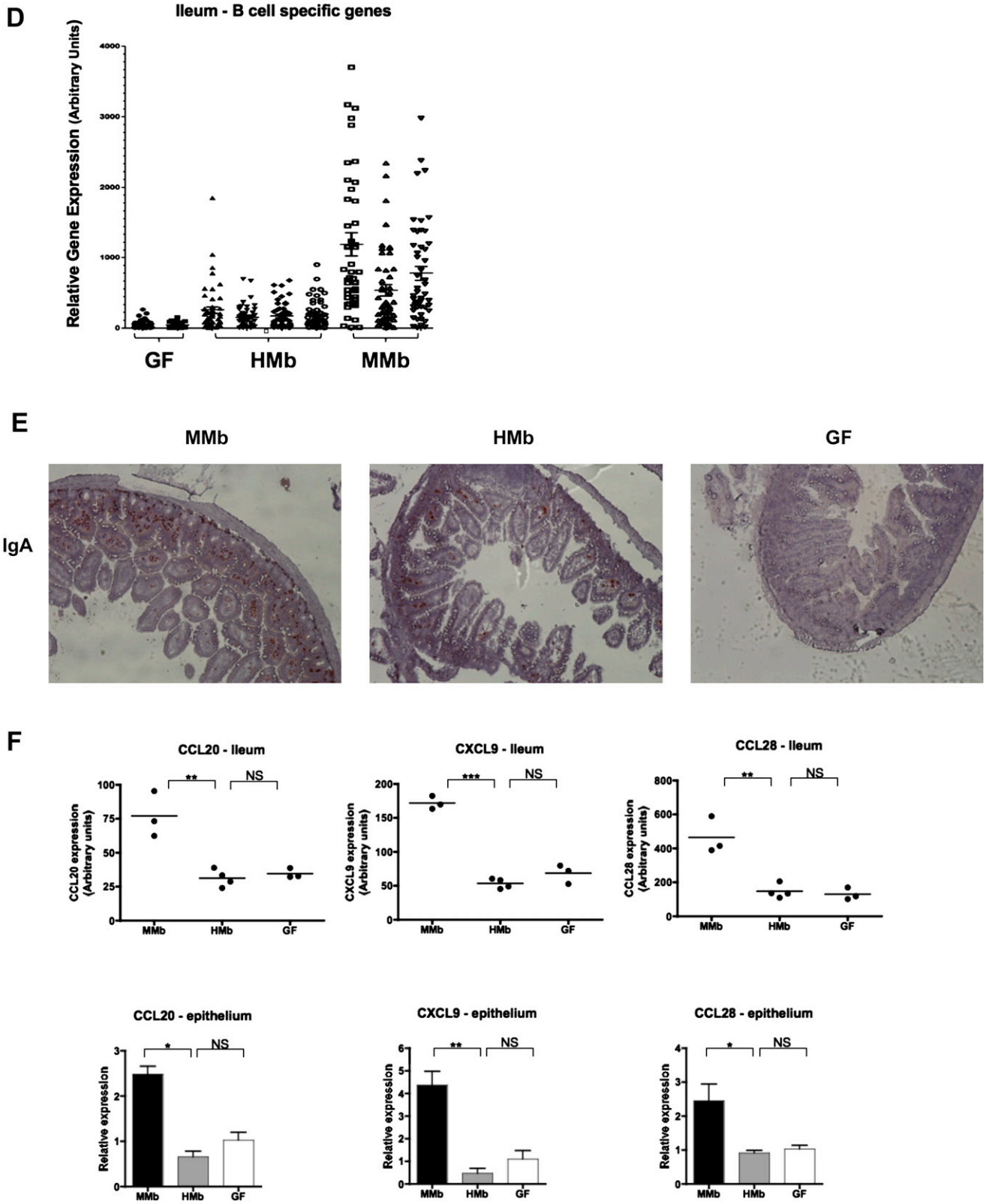

Figure S5. (*continued*).

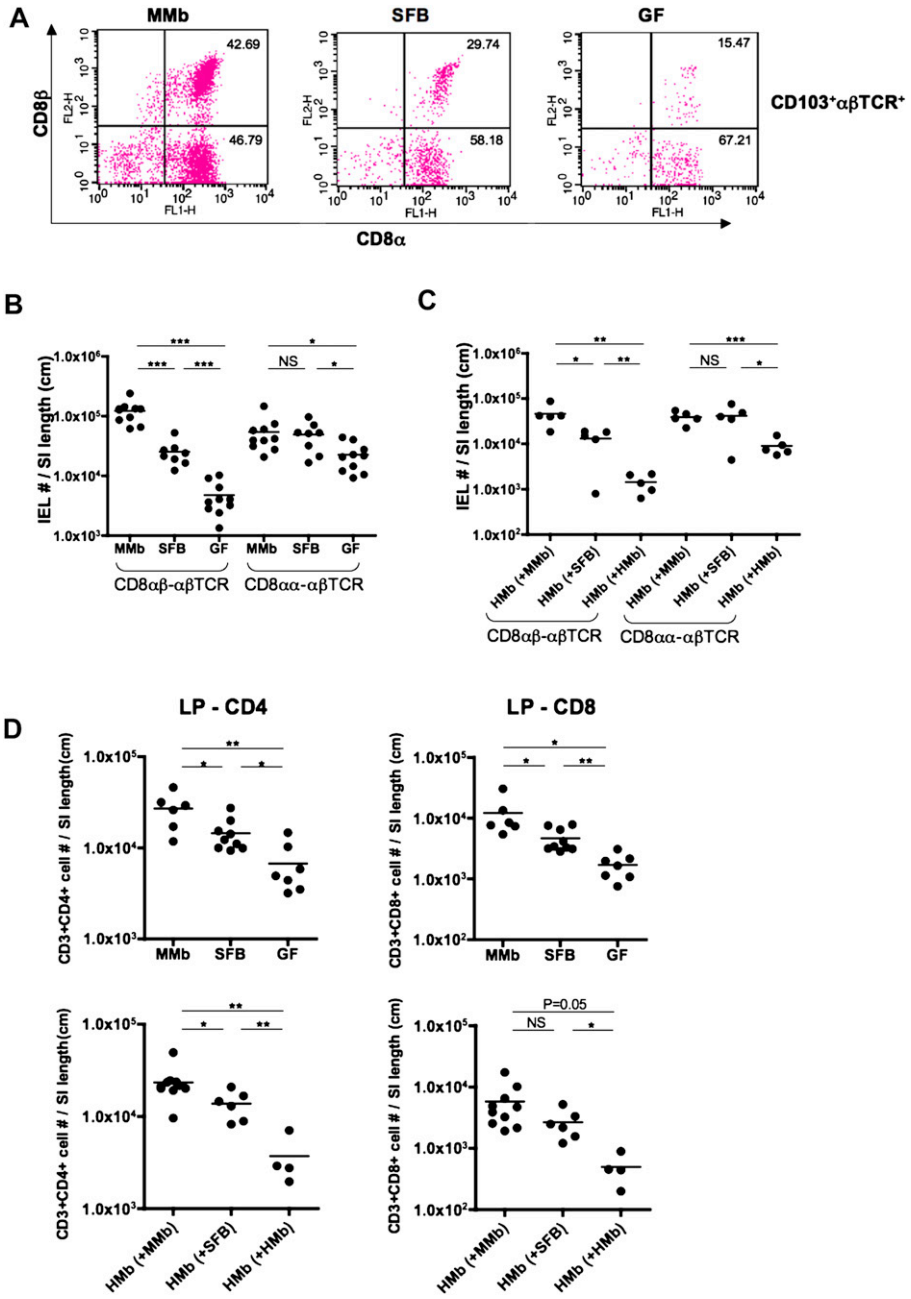

Figure S6. Segmented Filamentous Bacteria Partially Rescue Intestinal T Cell Numbers, Related to Figure 6

(A–C) IELs extracted from the small intestine were stained with fluorescently labeled antibodies to CD103, TCRβ, CD8α, and CD8β. CD8αβ-αβTCR IELs are $CD103^+\alpha\beta TCR^+CD8\alpha^+CD8\beta^+$ (*upper right quadrant*) and CD8αα-αβTCR IELs, $CD103^+\alpha\beta TCR^+CD8\alpha^+CD8\beta^-$ (*lower right quadrant*). Numbers indicate percentages of cells in the quadrant of $CD103^+\alpha\beta TCR^+$ cells (A). Absolute numbers of CD8αβ-αβTCR and CD8αα-αβTCR IELs normalized to small-intestinal length (cm) from: MMb, SFB-monocolonized, and GF mice (B); and HMb mice co-housed with MMb, SFB monocolonized, or HMb mice (C).

(D) After IEL extraction, remaining LP tissue was digested and analyzed by flow cytometry. Absolute numbers of $CD3^+CD4^+$ and $CD3^+CD8^+$ cells were normalized to small intestinal length (cm) from: MMb, SFB-monocolonized, and GF mice (*upper panel*); and HMb mice co-housed with MMb, SFB monocolonized, or HMb mice (*lower panel*).

(E) Abundance of SFB measured as SFB-specific 16S rDNA copy numbers by qPCR analysis of fecal pellets. SFB load was measured in HMb mice co-housed with SFB monocolonized or MMb mice. SFB abundance in MMb and HMb mice were analyzed as positive and negative controls, respectively.

(F and G) Single-cell suspensions of PPs were stained with fluorescently conjugated antibodies to CD3 and CD4, with subsequent intracellular staining with fluorescent antibodies to RORgt and Foxp3. Percentages of cells positive for RORgt and Foxp3 of $CD3^+CD4^+$ are presented in panels F and G, respectively. In panels B–H, each dot represents an individual mouse. Horizontal bars indicate the means. *P* values were calculated by unpaired/two-tailed t test. *p < 0.05, **p < 0.01, ***p < 0.001, NS = not significant by t test.

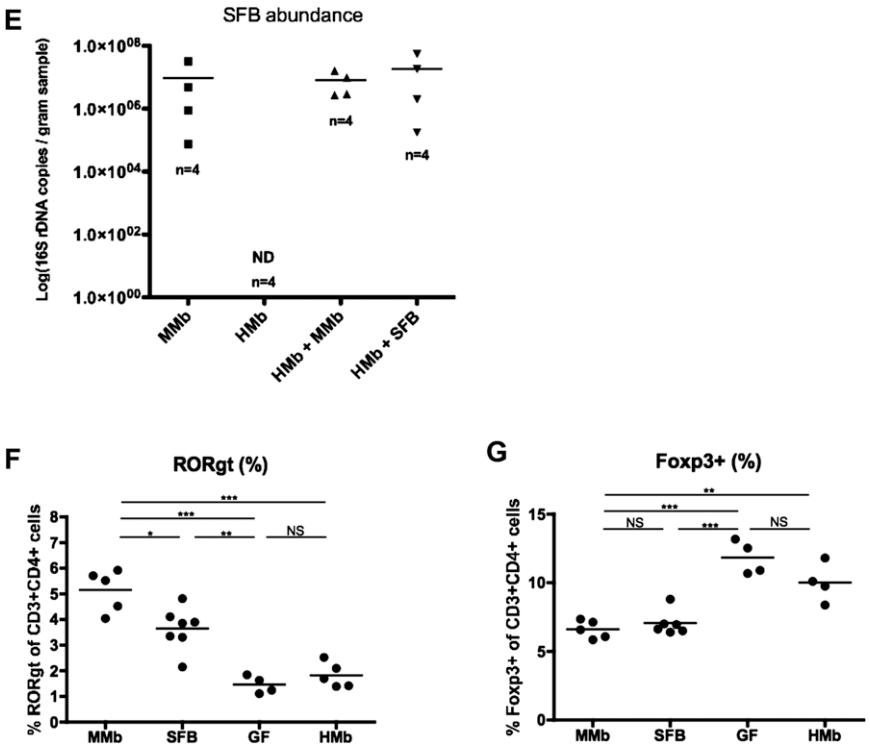

Figure S6. (*continued*).

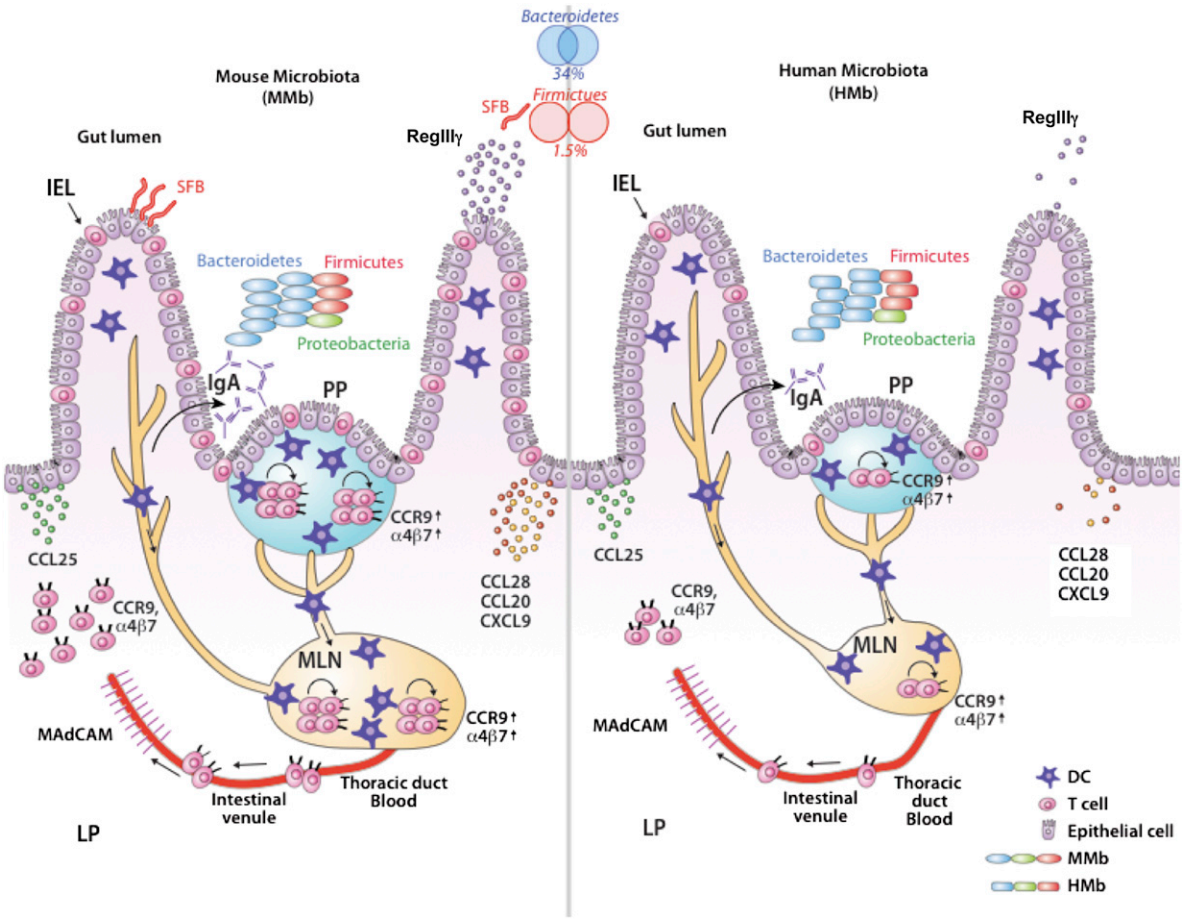

Figure S7. An Overview of the Regulation of the Mouse Small Intestinal Immune System by MMb versus HMb, Related to Table S3

Microbiota: In both MMb and HMb mice, Bacteroidetes were the most dominant phyla followed by Firmicutes, and Proteobacteria in the gut. Within the Bacteroidetes phyla, 34% of OTU (or bacterial species) were shared by both MMb and HMb. Among the OTUs within the Firmicutes, only 1.5% were shared by both MMb and HMb. SFB - a commensal bacterium and member of the Firmicutes - was detected in MMb, but not HMb - exemplifying host specificity within the Firmicutes phyla.

PP, MLN: Compared to MMb mice, HMb mice PP/MLN contains lower absolute numbers of DCs and T cells. The lower rate of T cell proliferation observed in HMb mice could contribute to the lower absolute number of small intestinal T cells in HMb mice. In both MMb and HMb mice, proliferating T cells in PP/MLN upregulate the intestinal homing receptors $\alpha4\beta7$ and CCR9.

LP: Proliferating T cells in the PP/MLN empty into the thoracic duct, enter the blood stream, and exit into the gut mucosa through intestinal venules in the small intestinal LP where MAdCAM and CCL25—ligands of $\alpha4\beta7$ and CCR9, respectively—are expressed. No differences were observed in the expression of MAdCAM and CCL25 between MMb and HMb mice. Due to low numbers of proliferating T cells originating from the HMb mice PP/MLN, the HMb mice small intestinal LP have lower numbers of T cells compared to MMb mice LP. A lower number of secretory IgA^+ cells were observed in the LP of HMb mice compared to the same compartment in MMb mice.

Epithelium: Low number of T cells in the small intestinal LP of HMb mice can lead to lower numbers of IELs embedded in the HMb mice epithelium, compared to the MMb epithelium. MMb mice epithelial cells, but not HMb epithelial cells, upregulate RegIIIγ an antimicrobial peptide. The expression of chemokines CCL20, CCL28, and CXCL9 are induced by MMb, but not HMb.